The Astronomical Journal, 141:170 (32pp), 2011 May doi:10.1088/0004-6256/141/5/170
© 2011. The American Astronomical Society. All rights reserved. Printed in the U.S.A.

ROTATIONAL PROPERTIES OF JUPITER TROJANS. I. LIGHT CURVES OF 80 OBJECTS

Stefano Mottola[1,9], Mario Di Martino[2], Anders Erikson[1], Maria Gonano-Beurer[1,3], Albino Carbognani[4], Uri Carsenty[1], Gerhard Hahn[1], Hans-Josef Schober[5], Felix Lahulla[6], Marco Delbò[7], and Claes-Ingvar Lagerkvist[8]
[1] DLR Institute of Planetary Research, Rutherfordstr. 2, DE-12489 Berlin, Germany; Stefano.Mottola@dlr.de
[2] INAF, Osservatorio Astronomico di Torino, Via Osservatorio 20, Pino Torinese, IT 10025 Torino, Italy
[3] Friedenstr. 12, 89073 Ulm, Germany
[4] Astronomical Observatory of the Autonomous Region of the Aosta Valley, Fraz. Lignan 39, 11020 Nus (AO), Italy
[5] Institut für Astronomie der Universität, Universitätsplatz 5, A-8010 Graz, Austria
[6] Observatorio Astronomico, Alfonso XII 3, 28014 Madrid, Spain
[7] UNS, CNRS, Observatoire de la Côte d'Azur, Nice, France
[8] Institutionen för Fysik och Astronomi, Uppsala Universitet, Box 516, S-75120 Uppsala, Sweden
Received 2010 August 30; accepted 2011 February 28; published 2011 April 7

ABSTRACT

We present the results of a Jupiter Trojans' light curve survey aimed at characterizing the rotational properties of Trojans in the approximate size range 60–150 km. The survey, which was designed to provide reliable and unbiased estimates of rotation periods and amplitudes, resulted in light curves for a total of 80 objects, 56 of which represent the first determinations published to date and nine of which supersede previously published erroneous values. Our results more than double the size of the existing database of rotational properties of Jovian Trojans in the selected size range. The analysis of the distributions of the rotation periods and light curve amplitudes is the subject of companion papers.

Key words: methods: data analysis – methods: observational – minor planets, asteroids: individual (Jupiter Trojans) – techniques: photometric

1. INTRODUCTION

Jovian Trojan asteroids are a population of objects co-orbital with Jupiter. Because of their greater distance and consequent fainter apparent magnitudes, these objects have been generally less frequently observed than main belt asteroids.

There are two groups of Jovian Trojans, each consisting of objects that librate about the Lagrangian equilateral stability points L4 and L5 of the Sun–Jupiter system, respectively, leading and trailing Jupiter by 60° in heliocentric ecliptic longitude. These objects have been demonstrated to be dynamically stable over the age of the solar system (Levison et al. 1997).

Because of their special location, Trojans are of particular interest and importance for understanding the origin and evolution of Jupiter and its system of inner (regular) and outer (irregular) satellites. The surface and internal compositions of the Trojans are expected to reflect the materials and conditions in the solar nebula at the time and location of their accretion.

As of 2010 August 20, there were 2800 known asteroids in the L4 group and 1757 in the L5 group.[10]

From a wide-field photographic survey centered on the leading Trojan cloud, and covering about 700 deg^2, Lagerkvist et al. (2000) estimated a population of about 1100 L4 Trojans down to a size of 17 km. By analyzing the serendipitous discoveries of Trojans during a trans-Neptunian object survey covering about 20 deg^2 Jewitt et al. (2000) estimated an L4 population of $\sim 1.6 \times 10^5$ down to a diameter of 2 km, with a combined mass of $\sim 10^{-4}$ Earth masses. The mean collision velocity in the Trojan clouds is about 5 km s^{-1}, similar to that in the main belt (Marzari et al. 1997; Dell'Oro et al. 1998, 2001). This similarity is due to the lower Keplerian velocities at the heliocentric distance of the Trojan clouds being compensated by the higher average orbital inclinations of the Trojans. The intrinsic collision probability for the Trojans is about twice that found in the main belt (Dell'Oro & Paolicchi 1998; Dell'Oro et al. 1998), which, contrary to what was commonly accepted earlier, leads to a picture of a Trojan population where considerable collisional evolution takes place. This scenario is further confirmed by the discovery of dynamical families among the Trojans (Milani 1993).

Shape and angular momentum are acquired during the accretion process, and are affected by the subsequent collisional evolution of the bodies. The characterization of these properties can provide important clues to the history of the Trojans. Light curve observations represent the basic tool for determining the rotational properties of asteroids, allowing for the determination of the rotation rate, rotational axis direction, and an estimate of the body shape. Some important physical properties, directly related to the outcome of collisional events, can be inferred from light curve observations.

Early work by Hartmann et al. (1988), Zappalà et al. (1989), and Binzel & Sauter (1992), the latter being based on a sample of 31 objects, suggested that Trojans might have a larger incidence of high-amplitude light curves, compared to main belt asteroids. Based on these data, the authors proposed that these objects may possess considerably elongated shapes, possibly reflecting a difference in composition and/or collisional evolution with respect to their counterparts in the main belt. In particular, Hartmann & Tholen (1990) proposed a similarity between Trojans and cometary nuclei, and hypothesized a mechanism of topography exaggeration by sublimation of volatiles, which could explain the elongated shapes of Trojans.

These initial investigations, however, were based on a limited sample and were affected by an observational bias tending to favor the determination of high amplitudes and short periods.

More recently, Mann et al. (2007) conducted a sparse-sampling photometric survey to perform a statistical investigation of the light curve amplitudes of Jovian Trojans which

[9] Author to whom any correspondence should be addressed.
[10] (http://www.cfa.harvard.edu/iau/lists/JupiterTrojans.html)

Table 1
Telescopes and Instruments

	Telescope	Instrument	Detector	Plate Scale (arcsec pixel^{-1})	Field of View (arcmin)
1	ESO, 61 cm Bochum	DLR MKII	Tek 1024 × 1024	0.54	9.2 × 9.2
2	ESO, 90 cm Dutch	CCD Camera 29	Tek 512 × 512	0.46	3.9 × 3.9
3	ESO, 1 m	DLR MKI	Thomson 384 × 576	0.35	2.2 × 3.4
3	ESO, 1 m	DLR MKI + focal red.	Thomson 384 × 576	0.54	3.5 × 5.2
4	ESO, 1 m	DLR MKII	Tek 1024 × 1024	0.30	5.2 × 5.2
5	Calar Alto, 1.2 m	CCD Camera 2b 17	SITe 2048 × 2048	0.46	15.8 × 15.8
6	Pino Torinese 1 m	SCAM-2	Loral 2048 × 2048	0.31	10.6 × 10.6
7	Loiano 1.52 m	DLR MKI	Thomson 384 × 576	0.50	3.2 × 4.8
7	Loiano 1.52 m	DLR MKI + focal red.	Thomson 384 × 576	0.77	5.0 × 7.4
8	Loiano 1.52 m	BFOSC	e2v 1340 × 1300	0.58	12.6 × 13.0
9	Kvistaberg 100/135 cm	DLR MKII	Tek 1024 × 1024	0.41	7.0 × 7.0
10	OAVdA 81 cm	FLI ProLine	Fairchild 2048 × 2048	0.97	16.5 × 16.5

was designed to detect possible large-amplitude contact binary candidates. In their work, the authors acquired five exposures for each object, for a total of 114 Trojans. Due to its own nature, however, the survey could only provide lower bounds for the amplitudes and produced period determinations for only two objects.

The necessity of determining a sizable, reliable, and unbiased sample of rotation periods and amplitudes has motivated our observational program to systematically explore the rotational properties of Trojans. For this reason we mostly selected targets brighter than an absolute magnitude $H = 10$ (or a diameter of about 60 km) and aimed at achieving a good degree of completeness down to this limit. The fact that the survey has been performed under uniform conditions also makes it easier to assess possible bias sources.

This paper reports the results of the light curve observations for 80 objects acquired in the course of this program over two decades. The analysis of the distributions of the rotation periods and light curve amplitudes is the subject of companion papers. Preliminary results from an earlier stage of this survey were also summarized in Barucci et al. (2002).

2. OBSERVATIONS

In order to determine the rotational properties of the target objects, we performed time-resolved CCD photometric series in the optical range. We used the technique of differential photometry, which makes use of field stars present in the same CCD frame as the target to allow for accurate removal of atmospheric extinction variability. Depending on the spectral sensitivity of the particular CCD used and on the instrumental setup, the observations were performed in the *V* and/or in the *R* spectral bands, aiming to maximize the signal-to-noise ratio (S/N) of the measurements.

The telescope was generally unguided, and tracked halfway between the rate of the object and the sidereal rate, in order to produce a similarly shaped point-spread function for both the target and the reference stars. The telescope fields were carefully centered to keep suitable reference stars within the CCD frame for the whole night.

The exposure times were chosen to produce an S/N between 80 and 150, which typically resulted in exposures between 1 and 5 minutes, the upper limit being determined by cosmic hits contamination and telescope guide errors. As no super-fast rotation is possible in the size range of the observed objects for any realistic material strength, even the longest exposures provide adequate sampling for any possible rotation period.

In general, whenever the telescope provided reliable pointing, we cycled between three and six objects per night, aiming to obtain an approximately uniform sampling at a rate of one data point every 15–30 minutes and the longest possible baseline. Whenever possible, the objects were then re-observed on subsequent nights, until a reliable period could be determined.

During nights of photometric quality, we acquired calibration sequences of the target objects and of photometric standard stars in the *V* band, in order to tie the observed magnitudes to the Johnson standard system. In addition to the Landolt Catalog (Landolt 1983), we used stars from the Guide Star Photometric Catalog (GSPC; Lasker et al. 1988) as photometric standards. Although the latter contains only tertiary standard stars, its advantage is a high density of stars throughout the celestial sphere, in a range of brightness well suited to CCD photometry. The use of the GSPC enabled us to select standard stars with solar-like colors located within only a few degrees of the target objects. As a consequence, these star fields were observed (generally close to their culmination) at air masses very close to those of the target objects, thereby minimizing the contribution of the error in the extinction coefficient on the determination of the absolute magnitude. Further, the similarity of the colors of the targets and of the standard stars made a color index correction unnecessary. The resulting accuracy of the absolute calibrations was typically in the range of 0.02–0.03 mag rms.

The observations were carried out using a number of different telescope and instrument combinations as detailed in Table 1.

3. DATA REDUCTION

The reduction of the CCD frames consisted of conventional dark removal and flat-fielding, which was performed by using high S/N dark and flat calibration frames. The flat fields were acquired by observing dithered sky fields during twilight and subsequently removing the field stars. Care was taken to use exposure times that were long enough that the shutter-induced exposure non-uniformity stayed below 0.5% from center to edge. Morning and evening flats were also compared to expose possible straylight contamination.

The source flux extraction was performed with AstPhot, a synthetic photometric aperture application developed at DLR (Mottola et al. 1995). Within AstPhot, the user interactively selects the comparison stars and the target object to be measured and defines the size and the shape of the synthetic apertures to be used (parameterized as an ellipse) and the regions to be used for the background estimation. In a case where the synthetic aperture of the target is different from those of the comparison stars (e.g., due to the adopted tracking rate), an aperture correction factor is introduced based on a photometric growth curve analysis. Typical aperture sizes used for these observations range from 5″ to 10″. The comparison stars were checked against each other to detect possible variability, and were then used to determine the atmospheric extinction. The resulting observed magnitudes (relative to the comparison stars, or, if calibrations were available, expressed in the Johnson system) were then reduced to unit distance from Earth and from the Sun. Furthermore, the times of the observations were light-travel subtracted, and a small correction for compensating the varying solar phase angle during the night applied, following the HG system.

The individual-night light curves were then merged into a composite by using the Fourier analysis procedure described in Harris et al. (1989). In this method, a light curve is approximated with a Fourier polynomial of the desired order. For each trial rotation period within a given range, a linear equation system is constructed, which is then least-squares fitted to the data to retrieve the best-fit Fourier coefficients and an individual night's magnitude shifts. A solution is achieved if a global minimum of the residuals in the chi-squared sense is found, under the assumption that the number of light curve extrema per cycle (usually, but not necessarily, two maxima and two minima) is known. One of the critical issues about the period determination is the presence of possible alias solutions, which can arise from a combination of causes such as inadequate sampling, incomplete coverage, commensurabilities with the Earth day length and light curves with an unusual number of extrema. A careful design of the observations helped us reduce some of these effects.

The possibility of having a quick-look data reduction capability at the telescope proved to be key to the success of the observations. In this way, it was possible to schedule the next night's observations in an efficient way by securing full coverage of the light curve, avoiding repetitions, and adjusting the exposure times, if necessary.

Table 2 reports the observational circumstances for the target objects. The date of observation is given to the tenth of the day closest to the mid-time of the observations. The following columns report the ecliptic longitude and latitude, the solar phase angle, the geocentric and heliocentric distances, the V magnitude reduced to 1 AU, the telescope and instrument combinations, and the observers, respectively.

The light curve data are reported in the figures in the form of composites as a function of the synodic rotational phase and with the light-travel corrected time of the zero phase reported in the legend. In the case of 7119 Hiera, in which it was not possible to determine a rotation period, the data are plotted as a function of the light-travel-corrected UT time. The synodic periods in each figure legend represent the periods used to compile the composite. So as not to compromise the legibility of the figures, we omit the error bars on the individual data points. The data points beyond rotational phase 1.0 are repeated for clarity.

The results are summarized in Table 3 in the form of synodic rotation periods and light curve amplitudes along with their 1σ uncertainties. We also assign a quality code to the reliability of the determinations by adopting the convention defined in Warner et al. (2009). The last column in Table 3 describes whether for each particular object our determination constitutes a new period (N) or we confirmed (C), refined (R), or superseded (S) a previously published value.

Diameters in Column 4 of Table 3 were assigned to the individual objects according to the availability and reliability of the respective sources. For this purpose, we adopted a hierarchical scheme in which the sources were used in the following order: (1) occultation results, (2) supplemental *IRAS* Minor Planet Survey from Tedesco et al. (2002), (3) average diameters from Fernandez et al. (2003), (4) the formula

$$D\,(\mathrm{km}) = 10^{(3.1236-0.2H-0.5\log(p_V))}$$

from Fowler & Chillemi (1992) with a geometric albedo $p_V = 0.05$ as the average albedo for the P and D taxonomic classes and the H value from the Minor Planet Center. The taxonomic types are taken from NASA's Planetary Data System database (Tedesco et al. 2004), from Lazzaro et al. (2004), and from Bus & Binzel (2002).

4. NOTES ON INDIVIDUAL OBJECTS

588 Achilles

There are several previously published determinations for this object which do not agree with each other. While Lagerkvist & Sjölander (1979) could not obtain a viable rotation period from observations during a single night in 1977, Zappalà et al. (1989) suggested a period longer than 12 hr from three nights' data in 1985. Angeli et al. (1999) derived a rotation period between 8.64 and 8.71 hr based on data obtained during four nights in 1995. More recently, Shevchenko et al. (2009) found a period of 7.306 hr from observations spanning from 2007 July to October plus two nights in 2008 September. Stephens (2010) determined a period of 7.312 hr, derived from data obtained in 2009 October. Our observations from two nights in 1994 July yield a rotation period of 7.32 ± 0.02 hr (see Figure 1), in good agreement with the last two studies.

659 Nestor

Four nights of observations in 1995 enabled us to measure a reliable rotation period of 15.98 ± 0.03 hr (see Figure 2). The previous estimate, reported by Binzel & Sauter (1992), and based on two nights in 1998, was inaccurate by almost an hour. Hartmann et al. (1988) reported only a light curve amplitude for the 1986 apparition. Quite surprisingly, our determination appears to be the first accurate period measurement published for this comparatively bright object.

884 Priamus

We observed this object during the apparitions of 1993 and 2001. The good sampling and coverage of the light curves resulted in a reliable period determination of about 6.9 hr (see Figures 3 and 4). This object was previously observed photometrically by Hartmann et al. (1988) during four different apparitions between 1983 and 1987. However, the authors reported amplitude estimates but no rotation periods.

911 Agamemnon

Early work by Dunlap & Gehrels (1969), Taylor (1971), and Binzel & Sauter (1992) suggested a rotation period of about 7 hr. More recently, Stephens (2009) found a more precise value of 6.592 ± 0.004 hr, which agrees very well with our determination from 1997 (see Figure 5).

Table 2
Observational Circumstances and Mean Magnitudes

Asteroid	UT Date		λ (deg J2000)	β (deg J2000)	α (deg)	r (AU)	Δ (AU)	$V(1, \alpha)$	Telescope and Instrument[a]	Observer
588 Achilles	1994 Jul	3.3	288.1	–6.2	1.6	5.8958	4.8903	8.64	1	Mottola
		4.3	288.0	–6.2	1.6	5.8954	4.8882		1	Mottola
659 Nestor	1995 Aug	19.2	305.5	–3.8	4.4	4.6546	3.6931	9.02	1	Mottola, Schober
		20.2	305.4	–3.7	4.6	4.6542	3.6989		1	Mottola, Schober
		21.2	305.3	–3.7	4.8	4.6539	3.7038		1	Mottola, Schober
		22.2	305.1	–3.7	5.0	4.6536	3.7098		1	Mottola, Schober
884 Priamus	1993 Jan	14.9	115.8	1.1	0.3	5.7227	4.7393		9	Mottola, Lagerkvist
		18.1	115.4	1.1	0.5	5.7216	4.7387		9	Mottola, Lagerkvist
		19.9	115.2	1.1	0.8	5.7210	4.7399		9	Mottola, Lagerkvist
	2001 Oct	16.9	46.9	10.5	4.5	5.4862	4.5689		6	Delbò, Mottola
		17.9	46.8	10.5	4.3	5.4869	4.5638		6	Delbò, Mottola
911 Agamemnon	1997 Nov	3.9	41.9	24.6	4.8	4.8897	3.9704		6	Di Martino, Mottola
		18.9	39.8	24.7	5.7	4.8879	4.0040		6	Di Martino, Mottola
		23.9	39.1	24.6	6.3	4.8874	4.0289		6	Di Martino, Mottola
1143 Odysseus	1994 Jun	3.3	293.6	3.3	6.7	5.7253	4.9218		1	Mottola
		4.3	293.5	3.3	6.5	5.7252	4.9114		1	Mottola
		5.3	293.4	3.3	6.4	5.7250	4.9012		1	Mottola
		13.3	292.8	3.4	5.2	5.7240	4.8280		1	Mottola, Erikson
1172 Aneas	1993 Feb	27.1	122.2	–17.1	6.4	5.6776	4.8806	8.88	4	Mottola, Di Martino
	1993 Mar	1.1	122.0	–17.1	6.7	5.6772	4.8987	8.87	4	Mottola, Di Martino
		2.1	121.9	–17.1	6.8	5.6770	4.9081	8.89	4	Mottola, Di Martino
1437 Diomedes	1994 Jul	12.3	314.3	–2.8	4.6	5.2783	4.3378		1	Mottola, Carsenty
		15.3	314.0	–2.7	4.1	5.2776	4.3188		1	Mottola, Carsenty
		16.3	313.9	–2.6	3.9	5.2774	4.3131		1	Mottola, Carsenty
1749 Telamon	1995 Aug	19.2	298.5	–4.5	4.7	5.6729	4.7561	10.00	1	Mottola, Schober
		20.2	298.4	–4.5	4.9	5.6725	4.7631		1	Mottola, Schober
		21.1	298.3	–4.4	5.1	5.6720	4.7704		1	Mottola, Schober
		25.1	297.9	–4.4	5.7	5.6702	4.8020	10.04	1	Mottola, Schober
1867 Deiphobus	1994 Feb	8.2	136.0	–18.8	3.5	5.3240	4.3820		4	Mottola, Erikson
		9.2	135.9	–18.9	3.5	5.3238	4.3828	8.91	4	Mottola, Erikson
		10.2	135.7	–18.9	3.6	5.3236	4.3838		4	Mottola, Erikson
		11.2	135.6	–18.9	3.6	5.3234	4.3852		4	Mottola, Erikson
		12.2	135.4	–19.0	3.7	5.3231	4.3870		4	Mottola, Erikson
		17.2	134.7	–19.1	4.2	5.3221	4.3999		4	Mottola, Erikson
		18.2	134.6	–19.1	4.3	5.3219	4.4034		4	Mottola, Erikson
1868 Thersites	1994 Jun	7.3	299.8	19.8	8.4	5.0776	4.3292		2	Mottola, Erikson
		9.3	299.7	19.8	8.2	5.0760	4.3086		2	Mottola, Erikson
		10.3	290.6	19.9	8.0	5.0752	4.2984		2	Mottola, Erikson
1873 Agenor	1994 Feb	4.2	150.0	–21.4	5.0	4.9148	4.0087	10.67	4	Mottola, Erikson
		6.2	149.8	–21.4	4.8	4.9137	4.0000		4	Mottola, Erikson
		7.2	149.6	–21.4	4.7	4.9132	3.9963		4	Mottola, Erikson
		8.2	149.5	–21.4	4.6	4.9127	3.9928		4	Mottola, Erikson
		9.2	149.3	–21.4	4.5	4.9122	3.9895	10.63	4	Mottola, Erikson
2207 Antenor	1989 Oct	3.2	12.4	–4.6	1.0	5.1217	4.1244	9.20	3	Di Martino, Gonano
		4.2	12.3	–4.6	0.9	5.1216	4.1241		3	Di Martino, Gonano
		5.2	12.2	–4.6	0.9	5.1214	4.1240		3	Di Martino, Gonano
		9.2	11.6	–4.6	1.2	5.1209	4.1270		3	Di Martino, Gonano
	1996 Apr	13.3	221.5	7.2	3.6	5.1691	4.2113		1	Mottola
		21.2	220.5	7.3	2.2	5.1700	4.1814		1	Mottola
		25.2	219.9	7.3	1.7	5.1704	4.1734		1	Mottola
2223 Sarpedon	1994 Feb	8.2	171.2	–16.0	6.3	5.1805	4.3438		4	Mottola, Erikson
		12.2	170.7	–16.1	5.7	5.1801	4.3122		4	Mottola, Erikson
		16.2	170.3	–16.1	5.1	5.1797	4.2849		4	Mottola, Erikson
		19.2	169.9	–16.1	4.6	5.1794	4.2673		4	Mottola, Erikson
	1996 Apr	11.2	237.6	3.4	6.6	5.1086	4.2646		1	Mottola
		15.2	237.2	3.5	6.0	5.1083	4.2285		1	Mottola
		20.2	236.7	3.7	5.0	5.1080	4.1892		1	Mottola
		24.2	236.2	3.8	4.3	5.1078	4.1625		1	Mottola
2241 Alcathous	1991 Dec	13.8	69.6	5.8	2.4	5.4299	4.4665		7	Mottola, Gonano
		15.8	69.3	5.7	2.7	5.4291	4.4731		7	Mottola, Gonano
		17.8	69.1	5.7	3.1	5.4283	4.4809		7	Mottola, Gonano
2260 Neoptolemus	1995 Aug	20.2	311.5	–16.5	4.2	5.1808	4.2300		1	Mottola, Schober
		21.2	311.4	–16.5	4.4	5.1805	4.2339	10.03	1	Mottola, Schober
	2002 Mar	11.9	163.8	21.4	4.1	5.2851	4.3536		8	Mottola
		12.9	163.6	21.4	4.2	5.2854	4.3557		8	Mottola

Table 2
(Continued)

Asteroid	UT Date		λ	β	α	r	Δ	V(1, α)	Telescope and	Observer
			(deg J2000)		(deg)	(AU)	(AU)		Instrument[a]	
		14.1	163.4	21.3	4.3	5.2858	4.3587		8	Mottola
2357 Phereclos	1994 Feb	10.2	156.7	–1.4	2.9	5.1898	4.2320		4	Mottola, Erikson
		11.2	156.6	–1.4	2.7	5.1894	4.2274		4	Mottola, Erikson
		12.3	156.5	–1.4	2.5	5.1891	4.2230		4	Mottola, Erikson
		14.2	156.2	–1.4	2.1	5.1884	4.2150	9.21	4	Mottola, Erikson
	2010 Jul	5.0	307.9	2.7	4.9	5.0395	4.1009		5	Mottola
		6.0	307.8	2.7	4.7	5.0398	4.0948		5	Mottola
		7.1	307.7	2.7	4.5	5.0400	4.0890		5	Mottola
		9.1	307.4	2.7	4.1	5.0406	4.0779		5	Mottola
		10.1	307.3	2.7	4.0	5.0408	4.0731		5	Mottola
		11.1	307.2	2.7	3.7	5.0411	4.0683		5	Mottola
		12.1	307.1	2.7	3.5	5.0413	4.0639		5	Mottola
2363 Cebriones	1994 Feb	10.2	172.6	–28.9	7.3	5.1649	4.3845		4	Mottola, Erikson
		11.2	172.4	–28.9	7.2	5.1646	4.3769		4	Mottola, Erikson
		12.2	172.3	–29.0	7.1	5.1644	4.3693		4	Mottola, Erikson
		13.2	172.2	–29.0	7.0	5.1641	4.3620		4	Mottola, Erikson
		14.2	172.1	–29.0	6.9	5.1638	4.3549	9.51	4	Mottola, Erikson
2456 Palamedes	1995 Aug	22.2	296.2	–7.3	6.0	5.3307	4.4550		1	Mottola, Schober
		26.1	295.8	–7.1	6.6	5.3286	4.4885	9.68	1	Mottola, Schober
		27.1	295.7	–7.1	6.8	5.3281	4.4975	9.64	1	Mottola, Schober
		28.1	295.7	–7.1	6.9	5.3276	4.5068		1	Mottola, Schober
2674 Pandarus	2001 Oct	21.9	29.7	–1.1	0.3	5.5182	4.5232		8	Delbò
2759 Idomeneus	1991 May	8.1	186.2	10.7	8.0	4.8240	4.0271		3	Mottola, Gonano
		10.1	186.0	10.7	8.4	4.8244	4.0481		3	Mottola, Gonano
		15.1	185.7	10.8	9.1	4.8252	4.1024		3	Mottola, Gonano
		17.0	185.6	10.8	9.4	4.8255	4.1254		3	Mottola, Gonano
	1992 Jun	1.2	225.1	23.5	6.7	4.9426	4.0724		3	Mottola, Gonano
		3.1	224.9	23.4	6.9	4.9434	4.0855		3	Mottola, Gonano
		4.1	224.8	23.4	7.0	4.9438	4.0927		3	Mottola, Gonano
	2010 Nov	4.1	69.1	–25.2	6.5	5.2936	4.4659		5	Mottola
		5.1	69.0	–25.2	6.3	5.2931	4.4591		5	Mottola
		6.2	68.9	–25.3	6.2	5.2926	4.4515		5	Mottola
		7.0	68.8	–25.3	6.1	5.2922	4.4464		5	Mottola
		12.0	68.1	–25.5	5.6	5.2900	4.4189		5	Mottola
		13.1	68.0	–25.6	5.5	5.2895	4.4145		5	Mottola
		14.1	67.9	–25.6	5.4	5.2891	4.4101		5	Mottola
2895 Memnon	1990 Nov	15.2	75.6	–30.1	6.9	4.9575	4.1330		3b	Mottola
		16.2	75.5	–30.1	6.8	4.9577	4.1280		3b	Mottola
		17.2	75.3	–30.1	6.7	4.9578	4.1233		3b	Mottola
2920 Automedon	1994 Jun	3.2	268.8	15.1	4.1	5.2834	4.3296		1	Mottola
		4.2	268.7	15.1	4.0	5.2833	4.3254		1	Mottola
		10.2	267.9	15.4	3.3	5.2829	4.3063		1	Mottola, Erikson
		12.2	267.6	15.5	3.2	5.2828	4.3022		1	Mottola, Erikson
3063 Makhaon	1994 Jun	4.3	304.9	2.1	8.4	5.4580	4.7678		1	Mottola
		5.3	304.9	2.2	8.2	5.4581	4.7553		1	Mottola
		6.3	304.8	2.2	8.1	5.4582	4.7439		1	Mottola
	2009 Dec	10.9	36.1	12.9	7.6	5.1655	4.4140	9.16	5	Mottola, Carsenty
		11.9	36.0	12.9	7.8	5.1654	4.4148	9.17	5	Mottola, Carsenty
		14.8	35.8	12.7	8.2	5.1637	4.4563		10	Carbognani
		15.8	35.8	12.7	8.3	5.1633	4.4673		10	Carbognani
		16.8	35.7	12.6	8.4	5.1628	4.4783		10	Carbognani
		17.8	35.7	12.6	8.5	5.1624	4.4897		10	Carbognani
		19.8	35.6	12.5	8.8	5.1615	4.5134		10	Carbognani
3240 Laocoon	1996 Apr	16.2	204.2	–2.9	0.7	5.3563	4.3542		1	Mottola
		18.2	204.0	–2.9	1.0	5.3545	4.3537		1	Mottola
3317 Paris	1990 Nov	12.2	79.1	–29.4	6.5	5.7191	4.9312		3b	Mottola
		13.2	78.9	–29.5	6.4	5.7196	4.9250		3b	Mottola
		14.2	78.8	–29.5	6.3	5.7202	4.9191		3b	Mottola
	1998 Jul	16.0	302.8	10.2	3.1	4.5615	3.5683		5	Lahulla, Mottola
		17.0	302.7	10.1	2.9	4.5618	3.5661		5	Lahulla, Mottola
		18.0	302.5	10.1	2.7	4.5620	3.5642		5	Lahulla, Mottola
		19.0	302.4	10.0	2.6	4.5623	3.5626		5	Lahulla, Mottola
		20.0	302.2	9.9	2.5	4.5625	3.5613		5	Lahulla, Mottola
3451 Mentor	1993 Feb	27.1	119.1	–23.7	7.4	5.4368	4.6915	8.82	4	Mottola, Di Martino
		28.1	119.0	–23.7	7.5	5.4369	4.7006	8.80	4	Mottola, Di Martino

Table 2
(Continued)

Asteroid	UT Date		λ (deg J2000)	β (deg J2000)	α (deg)	r (AU)	Δ (AU)	$V(1, \alpha)$	Telescope and Instrument[a]	Observer
	1998 Jul	16.0	290.1	29.2	6.0	4.7480	3.8361		5	Lahulla, Mottola
		17.0	289.9	29.2	6.0	4.7478	3.8367		5	Lahulla, Mottola
		18.0	289.8	29.2	6.1	4.7476	3.8376		5	Lahulla, Mottola
		19.0	289.6	29.1	6.1	4.7474	3.8387		5	Lahulla, Mottola
		20.0	289.5	29.1	6.1	4.7472	3.8400		5	Lahulla, Mottola
3548 Eurybates	1992 May	23.2	235.4	–2.2	1.3	5.5739	4.5681	9.97	3	Mottola, Gonano
		25.3	235.1	–2.3	1.7	5.5743	4.5732		3	Mottola, Gonano
		26.1	235.0	–2.3	1.9	5.5744	4.5742		3	Mottola, Gonano
		29.3	234.6	–2.3	2.5	5.5750	4.5853		3	Mottola, Gonano
3564 Talthybius	1994 Jun	8.3	291.6	–18.4	7.0	5.1498	4.3154		1	Mottola, Erikson
		9.3	291.5	–18.4	6.9	5.1501	4.3075		2	Mottola, Erikson
		10.3	291.4	–18.4	6.8	5.1504	4.2994		2	Mottola, Erikson
		11.3	291.3	–18.5	6.6	5.1507	4.2907	10.09	2	Mottola, Erikson
		12.3	291.2	–18.5	6.5	5.1509	4.2849		2	Mottola, Erikson
		14.3	291.0	–18.6	6.2	5.1515	4.2712		2	Mottola, Erikson
3708 1974 FV_1	1993 Feb	24.1	132.5	–6.8	3.9	5.8910	4.9735	9.83	4	Mottola, Di Martino
		25.2	132.3	–6.8	4.1	5.8916	4.9805	9.84	4	Mottola, Di Martino
		26.1	132.2	–6.8	4.3	5.8922	4.9876	9.86	4	Mottola, Di Martino
3793 Leonteus	1994 Jun	13.3	299.2	24.5	7.1	5.6335	4.8527		2	Mottola, Erikson
		15.2	299.0	24.6	6.9	5.6332	4.8357		2	Mottola, Erikson
	1994 Jul	5.2	296.9	25.2	4.9	5.6307	4.7163		1	Mottola, Erikson
		6.2	296.7	25.2	4.9	5.6305	4.7129	9.33	1	Mottola, Erikson
	1997 Oct	1.3	29.2	–2.2	4.1	5.0289	4.0825		1	Mottola
		5.3	28.7	–2.3	3.3	5.0262	4.0607		1	Mottola
		6.3	28.6	–2.4	3.1	5.0256	4.0559		1	Mottola
3794 Sthenelos	1995 Aug	22.2	305.3	–4.2	4.8	4.8050	3.8615		1	Mottola, Schober
		23.2	305.1	–4.1	5.1	4.8039	3.8674		1	Mottola, Schober
		25.1	304.9	–4.1	5.5	4.8018	3.8789	10.99	1	Mottola, Schober
		26.1	304.8	–4.1	5.7	4.8008	3.8849	11.00	1	Mottola, Schober
4007 Euryalos	1995 Aug	22.2	316.3	–10.1	3.0	5.3053	4.3253		1	Mottola, Schober
		23.2	316.1	–10.1	3.2	5.3049	4.3289		1	Mottola, Schober
		24.2	316.0	–10.1	3.3	5.3045	4.3325		1	Mottola, Schober
		25.1	315.9	–10.1	3.5	5.3042	4.3360	10.69	1	Mottola, Schober
4035 1986 WD	1991 May	6.0	206.1	–6.1	3.6	5.4671	4.5081		3	Mottola, Gonano
		7.1	206.0	–6.1	3.8	5.4673	4.5134		3	Mottola, Gonano
	2009 Oct	10.0	33.2	6.1	3.4	5.0465	4.0856		5	Mottola
		15.0	32.5	6.0	2.5	5.0451	4.0669		5	Mottola
		16.0	32.4	6.0	2.3	5.0448	4.0640		5	Mottola
4057 Demophon	1994 Jun	9.3	290.4	–3.3	5.3	5.8301	4.9469		2	Mottola, Erikson
		10.3	290.3	–3.3	5.2	5.8297	4.9378		2	Mottola, Erikson
		11.3	290.2	–3.4	5.0	5.8294	4.9294	10.56	2	Mottola, Erikson
		12.3	290.1	–3.4	4.9	5.8290	4.9215		2	Mottola, Erikson
		13.3	290.0	–3.4	4.7	5.8286	4.9128		2	Mottola, Erikson
		14.3	289.9	–3.4	4.6	5.8283	4.9055		2	Mottola, Erikson
4063 Euforbo	1992 May	31.2	227.0	20.2	5.1	5.7209	4.8220	9.167	3	Mottola, Gonano
	1992 Jun	1.2	226.9	20.2	5.2	5.7212	4.8281		3	Mottola, Gonano
4086 Podalirius	1991 May	8.1	217.5	7.5	2.1	5.7922	4.8019		3	Mottola, Gonano
		9.1	217.3	7.5	2.3	5.7925	4.8047		3	Mottola, Gonano
		10.2	217.2	7.4	2.4	5.7927	4.8078		3	Mottola, Gonano
4348 Poulydamas	1990 Dec	20.9	69.2	–5.4	4.0	4.9078	3.9733		7b	Mottola, Di Martino
		21.9	69.0	–5.4	4.2	4.9084	3.9793		7b	Mottola, Di Martino
		22.9	68.9	–5.4	4.4	4.9090	3.9864		7b	Mottola, Di Martino
4489 1988 AK	1995 Aug	27.1	302.0	–17.7	6.1	5.5597	4.7079	9.483	1	Mottola, Schober
		28.1	301.9	–17.7	6.2	5.5595	4.7149		1	Mottola, Schober
		29.1	301.8	–17.6	6.3	5.5592	4.7231		1	Mottola, Schober
		30.1	301.7	–17.6	6.5	5.5589	4.7325	9.583	1	Mottola, Schober
	2010 Oct	27.0	43.3	–20.0	4.3	5.0534	4.1194		5	Mottola
		28.0	43.1	–20.0	4.2	5.0531	4.1167		5	Mottola
		29.0	43.0	–20.0	4.1	5.0527	4.1143		5	Mottola
	2010 Nov	3.0	42.3	–19.8	3.8	5.0507	4.1066		5	Mottola
		4.0	42.1	–19.8	3.8	5.0504	4.1060		5	Mottola
		5.0	42.0	–19.8	3.8	5.0500	4.1056		5	Mottola
		7.0	41.7	–19.7	3.8	5.0492	4.1058		5	Mottola
		11.9	41.0	–19.5	4.1	5.0473	4.1114		5	Mottola
		12.9	40.8	–19.5	4.1	5.0469	4.1134		5	Mottola

Table 2
(Continued)

Asteroid	UT Date		λ (deg J2000)	β	α (deg)	r (AU)	Δ (AU)	$V(1, \alpha)$	Telescope and Instrument[a]	Observer
		13.9	40.7	–19.4	4.2	5.0465	4.1157		5	Mottola
4543 Phoinix	2009 Oct	23.9	53.3	18.3	6.0	4.6052	3.7092		10	Carbognani
		25.9	53.1	18.3	5.7	4.6051	3.6989		10	Carbognani
		30.0	52.5	18.4	5.1	4.6051	3.6811		10	Carbognani
	2009 Nov	10.9	50.8	18.6	4.0	4.6051	3.6565		10	Carbognani
		11.9	50.7	18.6	3.9	4.6052	3.6563		10	Carbognani
		20.9	49.3	18.6	4.3	4.6053	3.6676		10	Carbognani
		21.9	49.2	18.6	4.4	4.6054	3.6702		10	Carbognani
		26.8	48.5	18.5	5.0	4.6055	3.6880		10	Carbognani
	2009 Dec	11.9	46.7	18.0	7.4	4.6062	3.7840	10.41	5	Mottola, Carsenty
		12.9	46.6	18.0	7.6	4.6062	3.7916		5	Mottola, Carsenty
		14.9	46.4	17.9	7.9	4.6063	3.8087		10	Carbognani
		15.8	46.3	17.9	8.0	4.6064	3.8177		10	Carbognani
4709 Ennomos	1990 Dec	14.9	72.9	–0.8	1.9	5.1382	4.1655		7b	Mottola, Di Martino
		15.9	72.7	–0.8	2.1	5.1383	4.1687		7b	Mottola, Di Martino
		18.9	72.3	–1.0	2.7	5.1388	4.1802		7b	Mottola, Di Martino
		19.9	72.2	–1.0	2.9	5.1390	4.1845		7b	Mottola, Di Martino
		22.8	71.8	–1.2	3.6	5.1395	4.1996		7b	Mottola, Di Martino
4715 1989 TS_1	1991 Nov	29.0	76.8	21.9	4.5	5.1319	4.2160		7	Mottola, Di Martino
		29.8	76.6	21.9	4.4	5.1322	4.2141		7	Mottola, Di Martino
		30.9	76.5	22.0	4.4	5.1326	4.2124		7	Mottola, Di Martino
	1991 Dec	12.0	74.9	22.1	4.2	5.1368	4.2135		7	Mottola, Gonano
4722 Agelaos	2002 Dec	2.9	66.6	0.5	0.8	4.7879	3.8039		5	Mottola
		3.9	66.5	0.5	1.0	4.7885	3.8058		5	Mottola
4754 Panthoos	1994 Feb	13.3	172.9	3.2	5.3	5.1790	4.2907		4	Mottola, Erikson
		14.3	172.7	3.2	5.0	5.1790	4.2822	10.52	4	Mottola, Erikson
		15.3	172.6	3.3	4.9	5.1790	4.2759		4	Mottola, Erikson
		16.3	172.5	3.3	4.7	5.1791	4.2688		4	Mottola, Erikson
		17.3	172.4	3.3	4.5	5.1791	4.2621		4	Mottola, Erikson
		18.3	172.3	3.3	4.3	5.1791	4.2556		4	Mottola, Erikson
		19.3	172.2	3.4	4.1	5.1791	4.2494		4	Mottola, Erikson
4791 Iphidamas	1991 Dec	14.8	77.0	2.0	1.2	4.9669	3.9867		7	Mottola, Gonano
		15.8	76.8	2.0	1.4	4.9670	3.9886		7	Mottola, Gonano
	1993 Feb	27.1	105.0	–17.0	9.3	5.0451	4.4163	11.15	4	Mottola, Di Martino
		28.0	105.0	–17.0	9.4	5.0454	4.4282		4	Mottola, Di Martino
	1993 Mar	1.1	105.0	–17.0	9.5	5.0457	4.4417	11.13	4	Mottola, Di Martino
		2.1	104.9	–17.0	9.6	5.0460	4.4546	11.18	4	Mottola, Di Martino
4792 Lykaon	1996 Apr	12.3	220.4	4.8	3.3	5.5268	4.5663		1	Mottola
		13.3	220.3	4.8	3.1	5.5263	4.5608		1	Mottola
		15.2	220.0	4.8	2.7	5.5252	4.5508		1	Mottola
		16.3	219.9	4.7	2.6	5.5246	4.5460		1	Mottola
		18.2	219.7	4.7	2.2	5.5236	4.5377		1	Mottola
		19.3	219.5	4.7	2.0	5.5229	4.5336		1	Mottola
4805 Asteropaios	1994 Feb	10.2	155.8	–11.9	3.2	5.6313	4.6875		4	Mottola, Erikson
		13.2	155.4	–11.9	2.8	5.6324	4.6776		4	Mottola, Erikson
		14.2	155.3	–11.9	2.7	5.6329	4.6746	10.63	4	Mottola, Erikson
		16.2	155.0	–12.0	2.5	5.6336	4.6705		4	Mottola, Erikson
4827 Dares	1994 Feb	4.2	149.5	–9.4	3.2	5.1526	4.2021	10.99	4	Mottola, Erikson
		6.2	149.3	–9.4	2.9	5.1533	4.1953		4	Mottola, Erikson
		7.2	149.1	–9.4	2.7	5.1536	4.1923		4	Mottola, Erikson
		8.2	149.0	–9.5	2.6	5.1540	4.1897		4	Mottola, Erikson
		9.2	148.8	–9.5	2.4	5.1543	4.1871	10.98	4	Mottola, Erikson
4828 Misenus	1995 Apr	1.2	178.0	–2.5	2.6	5.0872	4.1097	10.96	1	Mottola
		2.2	177.9	–2.5	2.8	5.0875	4.1128		1	Mottola
		5.2	177.5	–2.6	3.4	5.0883	4.1260		1	Mottola
4832 Palinurus	2010 Jul	4.9	288.8	11.5	2.7	4.7878	3.7917		5	Mottola
		5.9	288.7	11.5	2.6	4.7869	3.7893		5	Mottola
		7.0	288.5	11.5	2.6	4.7860	3.7871		5	Mottola
		7.9	288.4	11.4	2.5	4.7851	3.7853		5	Mottola
		9.0	288.2	11.4	2.4	4.7842	3.7837		5	Mottola
		10.1	288.1	11.4	2.4	4.7832	3.7823		5	Mottola
		11.0	288.0	11.3	2.4	4.7824	3.7814		5	Mottola
		12.0	287.8	11.3	2.4	4.7815	3.7807		5	Mottola
4833 Meges	1995 Aug	27.1	299.2	–19.0	7.2	5.0503	4.2206	9.48	1	Mottola, Schober

Table 2
(Continued)

Asteroid	UT Date		λ (deg J2000)	β	α (deg)	r (AU)	Δ (AU)	$V(1, \alpha)$	Telescope and Instrument[a]	Observer
		28.1	299.1	–19.0	7.3	5.0497	4.2287		1	Mottola, Schober
		29.1	299.0	–19.1	7.4	5.0490	4.2372		1	Mottola, Schober
		30.1	298.9	–19.1	7.6	5.0484	4.2457	9.56	1	Mottola, Schober
4834 Thoas	1996 Sep	5.2	327.4	–33.6	6.6	5.1911	4.3465	9.73	1	Mottola, Carsenty
		6.2	327.2	–33.5	6.7	5.1900	4.3494		1	Mottola, Carsenty
		7.2	327.1	–33.5	6.8	5.1890	4.3523		1	Mottola, Carsenty
		8.2	327.0	–33.5	6.8	5.1880	4.3556		1	Mottola, Carsenty
4836 Medon	1991 May	8.2	211.2	18.0	4.5	5.1626	4.2240		3	Mottola, Gonano
		9.1	211.1	18.0	4.7	5.1633	4.2281		3	Mottola, Gonano
		10.3	210.9	17.9	4.8	5.1643	4.2344		3	Mottola, Gonano
		13.1	210.6	17.8	5.2	5.1666	4.2495		3	Mottola, Gonano
	1992 May	30.1	243.2	7.6	1.8	5.4595	4.4572	9.96	3	Mottola, Gonano
	2009 Dec	16.8	31.1	–15.1	9.3	5.0025	4.3744		10	Carbognani
		17.8	31.1	–15.0	9.4	5.0017	4.3860		10	Carbognani
		19.8	31.0	–14.9	9.6	5.0001	4.4100		10	Carbognani
	2010 Jan	10.8	31.2	–13.4	11.2	4.9826	4.7061		10	Carbognani
		11.8	31.3	–13.3	11.2	4.9818	4.7203		10	Carbognani
4946 Askalaphus	1992 May	23.2	240.8	–1.0	0.4	5.0355	4.0234	10.50	3	Mottola, Gonano
		25.3	240.5	–1.1	0.8	5.0353	4.0244	10.57	3	Mottola, Gonano
		26.1	240.4	–1.2	1.0	5.0352	4.0251		3	Mottola, Gonano
		29.2	239.9	–1.3	1.7	5.0348	4.0298	10.66	3	Mottola, Gonano
	1992 Jun	3.1	239.3	–1.5	2.7	5.0342	4.0431	10.64	3	Mottola, Gonano
		4.2	239.2	–1.5	3.0	5.0341	4.0467	10.63	3	Mottola, Gonano
5023 Agapenor	2009 Sep	18.9	19.1	13.3	5.2	4.9372	4.0169		5	Mottola
		21.0	18.8	13.3	4.9	4.9369	4.0060		5	Mottola
		22.1	18.7	13.4	4.7	4.9368	4.0003		5	Mottola
		25.1	18.3	13.4	4.2	4.9364	3.9873		5	Mottola
		26.0	18.2	13.5	4.0	4.9362	3.9834		5	Mottola
5025 1986 TS_6	2009 Oct	9.9	20.4	7.4	1.7	4.8911	3.9007		5	Mottola, Carsenty
		10.9	20.3	7.4	1.6	4.8907	3.8997		5	Mottola, Carsenty
		14.0	19.9	7.4	1.5	4.8895	3.8987		5	Mottola, Carsenty
		14.9	19.7	7.4	1.6	4.8892	3.8990		5	Mottola, Carsenty
		15.9	19.6	7.5	1.6	4.8888	3.8995		5	Mottola, Carsenty
	2009 Dec	10.9	14.9	7.6	10.5	4.8691	4.3576		5	Mottola, Carsenty
		11.9	14.9	7.6	10.6	4.8687	4.3720	11.09	5	Mottola, Carsenty
		12.8	14.9	7.6	10.7	4.8684	4.3856	11.11	5	Mottola, Carsenty
5027 Androgeos	1992 May	30.2	240.0	12.0	2.7	5.6165	4.6310		3	Mottola, Gonano
		31.1	239.9	12.0	2.8	5.6165	4.6333	10.06	3	Mottola, Gonano
	1992 Jun	3.2	239.5	11.8	3.2	5.6166	4.6424		3	Mottola, Gonano
5028 Halaesus	1996 Sep	5.2	353.7	–21.7	4.9	4.8740	3.9367	10.78	1	Mottola, Carsenty
		6.2	353.6	–21.7	4.8	4.8732	3.9333		1	Mottola, Carsenty
		7.2	353.4	–21.7	4.7	4.8723	3.9303		1	Mottola, Carsenty
		17.4	351.9	–21.5	4.4	4.8631	3.9149		1	Mottola, Carsenty
		19.3	351.7	–21.4	4.4	4.8614	3.9153		1	Mottola, Carsenty
		22.2	351.3	–21.3	4.6	4.8589	3.9177		1	Mottola, Carsenty
5119 1988 RA_1	1994 Feb	13.2	156.2	–5.8	2.3	5.7618	4.7962		4	Mottola, Erikson
		14.2	156.1	–5.8	2.1	5.7618	4.7924	10.74	4	Mottola, Erikson
		17.2	155.7	–5.9	1.6	5.7617	4.7845		4	Mottola, Erikson
5120 Bitias	1993 Feb	27.1	128.5	–9.4	5.0	5.8658	4.9979	10.87	4	Mottola, Di Martino
		28.1	128.4	–9.4	5.2	5.8659	5.0060	10.85	4	Mottola, Di Martino
	1993 Mar	1.1	128.3	–9.4	5.4	5.8659	5.0144	10.86	4	Mottola, Di Martino
		2.2	128.2	–9.4	5.5	5.8659	5.0246	10.83	4	Mottola, Di Martino
5130 Ilioneus	1994 Feb	4.2	139.0	–18.6	3.5	5.3262	4.3843	10.21	4	Mottola, Erikson
		6.2	138.7	–18.6	3.4	5.3262	4.3826		4	Mottola, Erikson
		7.2	138.6	–18.6	3.4	5.3262	4.3823		4	Mottola, Erikson
		8.2	138.5	–18.6	3.4	5.3263	4.3822		4	Mottola, Erikson
		10.2	138.2	–18.7	3.4	5.3263	4.3830		4	Mottola, Erikson
5144 Achates	1996 Apr	12.1	170.3	–5.7	5.6	5.5170	4.6460		1	Mottola
		13.1	170.2	–5.7	5.8	5.5150	4.6528		1	Mottola
		14.1	170.1	–5.7	5.9	5.5131	4.6593		1	Mottola
5254 Ulysses	1996 Sep	5.2	337.8	–29.7	5.8	5.0387	4.1409	9.80	1	Mottola, Carsenty
		6.2	337.6	–29.7	5.8	5.0378	4.1416		1	Mottola, Carsenty
		7.2	337.5	–29.7	5.8	5.0369	4.1425		1	Mottola, Carsenty
		8.2	337.3	–29.7	5.9	5.0360	4.1436		1	Mottola, Carsenty
		9.2	337.2	–29.7	5.9	5.0351	4.1451		1	Mottola, Carsenty

Table 2
(Continued)

Asteroid	UT Date		λ (deg J2000)	β	α (deg)	r (AU)	Δ (AU)	V(1, α)	Telescope and Instrument[a]	Observer
5259 Epeigeus	1995 Aug	26.2	334.6	−19.8	3.9	5.0197	4.0576	10.85	1	Mottola, Schober
		27.2	334.4	−19.8	3.9	5.0202	4.0579		1	Mottola, Schober
		28.2	334.3	−19.8	3.9	5.0207	4.0586		1	Mottola, Schober
		29.2	334.1	−19.8	3.9	5.0212	4.0595		1	Mottola, Schober
		30.1	334.0	−19.8	3.9	5.0217	4.0607	10.85	1	Mottola, Schober
5264 Telephus	1994 Jun	11.3	297.1	8.4	6.2	5.7640	4.9275	10.15	2	Mottola, Erikson
		12.3	297.0	8.4	6.1	5.7642	4.9184		2	Mottola, Erikson
		13.3	296.9	8.4	5.9	5.7643	4.9091		2	Mottola, Erikson
		14.3	296.8	8.3	5.8	5.7645	4.9001		2	Mottola, Erikson
5283 Pyrrhus	1996 Sep	5.2	332.0	−21.4	4.6	5.0996	4.1615	10.13	1	Mottola, Carsenty
	2002 Mar	12.1	178.4	20.6	3.9	5.3527	4.4169		5	Mottola
		13.1	178.2	20.6	3.9	5.3538	4.4160		5	Mottola
		14.1	178.1	20.6	3.8	5.3549	4.4154		5	Mottola
		19.1	177.4	20.6	3.7	5.3603	4.4168	10.07	5	Mottola
5476 1989 TO_{11}	1994 Feb	7.2	135.1	−14.9	2.7	5.4804	4.5223		4	Mottola, Erikson
		12.1	134.5	−14.8	3.0	5.4793	4.5282		4	Mottola, Erikson
		13.2	134.3	−14.8	3.1	5.4790	4.5303		4	Mottola, Erikson
		17.1	133.8	−14.7	3.6	5.4782	4.5419		4	Mottola, Erikson
5511 Cloanthus	2010 Jul	5.1	311.5	10.3	6.4	4.6199	3.7137		5	Mottola
		6.1	311.4	10.3	6.2	4.6201	3.7069		5	Mottola
		7.0	311.3	10.3	6.0	4.6202	3.7003		5	Mottola
		9.1	311.0	10.3	5.6	4.6206	3.6875		5	Mottola
		10.0	310.9	10.3	5.4	4.6208	3.6820		5	Mottola
		11.1	310.8	10.3	5.2	4.6210	3.6759		5	Mottola
		12.0	310.7	10.3	5.0	4.6212	3.6712		5	Mottola
5638 Deikoon	1994 Feb	8.2	138.9	−4.0	0.7	5.4068	4.4222		4	Mottola, Erikson
		9.2	138.8	−3.9	0.8	5.4061	4.4215	10.84	4	Mottola, Erikson
		15.2	138.0	−3.8	1.7	5.4015	4.4239		4	Mottola, Erikson
		16.2	137.9	−3.8	1.8	5.4007	4.4254		4	Mottola, Erikson
		18.2	137.6	−3.8	2.2	5.3992	4.4294		4	Mottola, Erikson
		19.2	137.5	−3.8	2.4	5.3984	4.4318		4	Mottola, Erikson
5648 1990 VU_1	2009 May	24.9	226.0	10.7	3.8	5.3529	4.3934		5	Mottola
		25.9	225.8	10.7	4.0	5.3517	4.3968		5	Mottola
		27.0	225.7	10.6	4.2	5.3504	4.4010		5	Mottola
		27.9	225.6	10.6	4.3	5.3493	4.4046		5	Mottola
		28.9	225.5	10.6	4.5	5.3482	4.4087		5	Mottola
		29.9	225.3	10.5	4.6	5.3470	4.4132		5	Mottola
	2009 Jun	16.9	223.6	9.6	7.5	5.3254	4.5383		5	Mottola
		18.9	223.4	9.5	7.8	5.3229	4.5575		5	Mottola
6002 1988 RO	1993 Feb	23.2	137.4	−17.6	4.3	5.4924	4.5765	10.98	4	Mottola, Di Martino
		25.2	137.1	−17.6	4.5	5.4934	4.5866	11.00	4	Mottola, Di Martino
		26.2	137.0	−17.5	4.7	5.4939	4.5920	11.02	4	Mottola, Di Martino
6090 1989 DJ	1994 Jun	11.3	300.4	−14.1	7.3	5.3816	4.5853	10.09	2	Mottola, Erikson
		12.3	300.3	−14.1	7.2	5.3812	4.5762		2	Mottola, Erikson
		13.3	300.3	−14.1	7.0	5.3808	4.5652		2	Mottola, Erikson
		14.3	300.3	−14.1	6.9	5.3804	4.5553		2	Mottola, Erikson
		15.3	300.3	−14.1	6.7	5.3800	4.5466		2	Mottola, Erikson
	2009 Sep	19.0	31.8	20.4	7.5	5.0145	4.2068		5	Mottola
		21.1	31.6	20.5	7.2	5.0143	4.1916		5	Mottola
		22.1	31.5	20.6	7.1	5.0142	4.1829		5	Mottola
		25.1	31.2	20.7	6.7	5.0138	4.1621		5	Mottola
		26.0	31.1	20.8	6.5	5.0137	4.1553		5	Mottola
	2009 Oct	10.0	29.4	21.4	4.8	5.0123	4.0882		5	Mottola
7119 Hiera	2009 Jul	17.1	8.3	19.8	11.8	4.8023	4.4341		5	Mottola
		18.1	8.3	19.9	11.7	4.8017	4.4199		5	Mottola
		19.1	8.4	20.0	11.7	4.8010	4.4058		5	Mottola
		20.0	8.4	20.0	11.6	4.8004	4.3916		5	Mottola
		21.1	8.4	20.1	11.6	4.7998	4.3778		5	Mottola
7641 1986 TT_6	2009 Sep	19.0	31.3	27.2	7.6	5.2042	4.4285		5	Mottola
		21.0	31.1	27.3	7.4	5.2034	4.4124		5	Mottola
		22.1	31.0	27.3	7.3	5.2029	4.4032		5	Mottola
		25.0	30.6	27.3	6.9	5.2018	4.3818		5	Mottola
		26.1	30.5	27.3	6.8	5.2014	4.3747		5	Mottola
	2009 Oct	14.0	27.9	26.9	5.1	5.1940	4.2910		5	Mottola

Table 2
(Continued)

Asteroid	UT Date		λ	β	α	r	Δ	V(1, α)	Telescope and Instrument[a]	Observer
			(deg J2000)		(deg)	(AU)	(AU)			
9799 1996 RJ	2009 Oct	10.0	36.2	28.9	6.6	4.9466	4.0903		5	Mottola
		11.0	36.0	28.9	6.5	4.9467	4.0860		5	Mottola
		12.0	35.9	28.8	6.4	4.9468	4.0818		5	Mottola
		12.9	35.7	28.8	6.3	4.9469	4.0779		5	Mottola
		14.0	35.6	28.8	6.2	4.9470	4.0741		5	Mottola
		16.0	35.3	28.8	6.0	4.9472	4.0679		5	Mottola
11395 1998 XN_{77}	2009 Dec	10.8	35.6	−5.3	7.7	5.0844	4.3245	10.35	5	Mottola
		11.9	35.6	−5.3	7.8	5.0849	4.3364	10.38	5	Mottola
		12.8	35.5	−5.3	7.9	5.0854	4.3471		5	Mottola
	2010 Nov	4.1	75.6	−17.6	6.7	5.2494	4.4323		5	Mottola
		5.1	75.5	−17.6	6.5	5.2499	4.4244		5	Mottola
		6.2	75.4	−17.7	6.4	5.2505	4.4160		5	Mottola
		7.0	75.3	−17.8	6.3	5.2509	4.4102		5	Mottola
		12.1	74.7	−18.1	5.5	5.2534	4.3783		5	Mottola
		13.1	74.6	−18.1	5.4	5.2539	4.3728		5	Mottola
		14.1	74.5	−18.2	5.3	5.2544	4.3678		5	Mottola
11509 Thersilochos	2010 Jul	4.9	271.3	20.1	4.7	4.8099	3.8579		5	Mottola
		5.9	271.1	20.1	4.8	4.8090	3.8598		5	Mottola
		6.9	271.0	20.1	5.0	4.8079	3.8621		5	Mottola
		9.9	270.6	20.1	5.3	4.8049	3.8707		5	Mottola
		10.9	270.5	20.1	5.5	4.8039	3.8740		5	Mottola
		11.9	270.3	20.1	5.6	4.8029	3.8777		5	Mottola
12929 1999 TZ_1	2009 May	30.0	275.8	49.4	9.4	5.0886	4.4347		5	Mottola
		31.1	275.6	49.5	9.3	5.0883	4.4295		5	Mottola
	2009 Jun	1.1	275.5	49.6	9.3	5.0881	4.4254		5	Mottola
		17.1	272.7	50.7	8.9	5.0843	4.3831		5	Mottola
		19.0	272.3	50.7	8.9	5.0838	4.3813		5	Mottola
		20.1	272.1	50.8	8.9	5.0835	4.3806		5	Mottola
		21.1	271.9	50.8	8.9	5.0833	4.3801		5	Mottola
16974 1998 WR_{21}	2009 Oct	10.0	23.9	12.1	2.9	4.8403	3.8655		5	Mottola
		10.9	23.8	12.1	2.8	4.8403	3.8640		5	Mottola
		11.9	23.6	12.0	2.7	4.8404	3.8628		5	Mottola
		12.9	23.5	12.0	2.6	4.8404	3.8618		5	Mottola
		14.0	23.3	12.0	2.5	4.8404	3.8611		5	Mottola
		14.9	23.2	12.0	2.5	4.8405	3.8608		5	Mottola
		15.9	23.1	12.0	2.4	4.8405	3.8607		5	Mottola
20729 1999 XS_{143}	2009 Oct	11.0	39.2	27.0	6.6	4.8680	4.0091		5	Mottola
		12.0	39.1	27.1	6.5	4.8679	4.0043		5	Mottola
		12.9	38.9	27.1	6.4	4.8679	3.9999		5	Mottola
		14.0	38.3	27.2	6.3	4.8679	3.9954		5	Mottola
		14.9	38.7	27.2	6.2	4.8678	3.9917		5	Mottola
21900 1999 VQ_{10}	2009 Oct	11.9	17.1	9.2	1.8	5.0420	4.0546		5	Mottola
		12.9	17.0	9.2	1.9	5.0418	4.0551		5	Mottola

Note. [a] For telescope/instrument description see Table 1.

1143 Odysseus

From our observations spanning four nights in 1994 June we determine a reliable rotation period of 10.111 ± 0.004 hr (see Figure 6), which is in agreement with the determination by Molnar et al. (2008).

1172 Aneas

Three nights of observations enabled us to determine an unambiguous rotation period of about 8.7 hr (see Figure 7). For this object only a previous amplitude estimation from the 1986 apparition was published (Hartmann et al. 1988).

1437 Diomedes

We observed this object for a total of about 22 hr during three nights in 1994 and measured only a slight intensity variation. Sato et al. (2000), in the course of their coordinated occultation campaign in 1997, derived a rotation period of 24.46 hr, an amplitude of 0.70 mag, and a triaxial shape of 284 × 126 × 65 km. We used their period, later confirmed by Stephens (2009), to produce a composite of our data, as shown in Figure 8. Although our data cover as much as 40% of the rotation period, the maximum intensity variation displayed by the observations was only about 0.02 mag. From the shape of the light curve we subjectively estimate that the maximum amplitude during the 1994 apparition had not exceeded 0.1 mag.

1749 Telamon

Four nights of observations in 1995 August resulted in a reliable rotation period of about 11.12 hr (see Figure 9). No previous period determinations are reported in the literature.

Table 3
Results

Asteroid	Trojan Cloud/ Family[a]	*H*	Estimated Diameter (km) and Source	Taxa	Syn. Period (hr)	Observed Amplitude	Apparition	Quality Code	Status
588 Achilles	L4	8.67	150 c	DU	7.32 ± 0.02	0.31 ± 0.01	1994	3	C
659 Nestor	L4	8.99	109 b	XC	15.98 ± 0.03	0.31 ± 0.01	1995	3	S
884 Priamus	L5	8.81	128 c	D	6.866 ± 0.004	0.27 ± 0.01	1993	3	N
					6.894 ± 0.020	0.26 ± 0.01	2001		
911 Agamemnon	L4	7.89	179 c	D	6.5819 ± 0.0007	0.29 ± 0.01	1997	3	C
1143 Odysseus	L4	7.93	124 c	D	10.111 ± 0.004	0.22 ± 0.01	1994	3	C
1172 Aneas	L5-A	8.33	140 c	D	8.708 ± 0.009	0.27 ± 0.01	1993	3	N
1437 Diomedes	L4	8.30	132 a	DP	–	$0.02 < a < 0.1$	1994	–	C
1749 Telamon	L4-M	9.2	74 c		11.187 ± 0.008	0.10 ± 0.01	1995	3	N
1867 Deiphobus	L5-D	8.68	127 c	D	58.66 ± 0.18	0.27 ± 0.03	1994	3	N
1868 Thersites	L4	9.3	82 d		10.416 ± 0.014	0.14 ± 0.01	1994	3	N
1873 Agenor	L5	10.5	47 d		20.60 ± 0.03	0.08 ± 0.01	1994	3	N
2207 Antenor	L5	8.89	86 c	D	7.977 ± 0.004	0.19 ± 0.01	1989	3	N
					7.965 ± 0.002	0.09 ± 0.01	1996		
2223 Sarpedon	L5-A	9.41	95 b	DU	22.77 ± 0.04	0.11 ± 0.01	1994	3	N
					22.741 ± 0.014	0.14 ± 0.01	1996		
2241 Alcathous	L5	8.64	108 c	D	7.687 ± 0.005	0.23 ± 0.01	1991	3	S
2260 Neoptolemus	L4	9.31	72 b	DTU	8.180 ± 0.022	0.20 ± 0.01	1995	3	R
					8.180 ± 0.008	0.32 ± 0.01	2002		
2357 Phereclos	L5-Ph	8.94	106 c	D	14.466 ± 0.020	0.06 ± 0.01	1994	3	N
					14.394 ± 0.012	0.09 ± 0.01	2010		
2363 Cebriones	L5	9.11	86 c	D	20.05 ± 0.04	0.22 ± 0.01	1994	3	C
2456 Palamedes	L4	9.6	92 b		7.258 ± 0.004	0.05 ± 0.01	1995	3	C
2674 Pandarus	L5	9.0	98 c	D	–	0.01 ± 0.01	2001	–	C
2759 Idomeneus	L4	9.8	65 d		–	>0.24	1991	3	N
					–	0.22 ± 0.02	1992		
					32.38 ± 0.06	0.27 ± 0.01	2010		
2895 Memnon	L5	9.9	62 d		7.502 ± 0.010	0.22 ± 0.01	1990	3	C
2920 Automedon	L4	8.8	120 c	D	10.220 ± 0.004	0.12 ± 0.01	1994	3	C
3063 Makhaon	L4-M	8.6	117 c	D	8.648 ± 0.014	0.09 ± 0.01	1994	2	S
					8.6354 ± 0.0033	0.06 ± 0.01	2009		
3240 Laocoon	L5	10.1	57 d		11.312 ± 0.024	0.55 ± 0.02	1996	3	N
3317 Paris	L5	8.4	113 c	T	7.082 ± 0.003	0.08 ± 0.01	1990	3	C
					7.082 ± 0.004	0.10 ± 0.01	1998		
3451 Mentor	L5	8.4	114 c	X	7.675 ± 0.019	0.18 ± 0.01	1993	3	C
					7.700 ± 0.005	0.15 ± 0.01	1998		
3548 Eurybates	L4-M	9.50	72 b		8.711 ± 0.009	0.20 ± 0.01	1992	3	C
3564 Talthybius	L4-Ta	9.3	69 b		40.59 ± 0.13	0.38 ± 0.01	1994	3	C
3708 1974 FV$_1$	L5	9.2	88 c		6.553 ± 0.008	0.23 ± 0.01	1993	3	N
3793 Leonteus	L4-T	8.8	86 b	D	5.6225 ± 0.0005	0.24 ± 0.01	1994	3	S
					5.618 ± 0.002	0.06 ± 0.01	1997		
3794 Sthenelos	L4	9.9	62 d		12.877 ± 0.016	0.27 ± 0.01	1995	3	N
4007 Euryalos	L4-M	10.3	52 d		6.391 ± 0.005	0.07 ± 0.01	1995	3	N
4035 1986 WD	L4-WD	9.3	82 d		13.52 ± 0.08	>0.20	1991	3	N
					13.467 ± 0.013	0.21 ± 0.01	2009		
4057 Demophon	L4-P	9.6	71 d		29.31 ± 0.07	0.23 ± 0.01	1994	3	N
4063 Euforbo	L4	8.6	113 d	D	8.841 ± 0.025	0.19 ± 0.01	1992	3	N
4086 Podalirius	L4-T	9.1	90 d		10.43 ± 0.04	0.13 ± 0.01	1991	3	S
4348 Poulydamas	L5-Po	9.2	86 d		9.908 ± 0.018	0.21 ± 0.01	1990	3	N
4489 1988 AK	L4	9.1	103 c	D	–	$\geqslant$0.04	1995	3	N
					12.582 ± 0.004	0.22 ± 0.01	2010		
4543 Phoinix	L4	9.7	68 d		38.866 ± 0.012	$\geqslant$0.34	2009	3	N
4709 Ennomos	L5-D	8.6	77 c		12.275 ± 0.008	0.47 ± 0.01	1990	3	N
4715 1989 TS$_1$	L5-A	9.6	71 d		8.8129 ± 0.0025	0.46 ± 0.01	1991	3	N
4722 Agelaos	L5	9.7	68 d		18.61 ± 0.12	0.23 ± 0.02	2002	2	N
4754 Panthoos	L5-An	10.0	59 d		27.68 ± 0.05	0.09 ± 0.01	1994	3	N
4791 Iphidamas	L5	9.9	62 d		9.57 ± 0.05	0.16 ± 0.01	1991	3	N
					9.727 ± 0.011	0.49 ± 0.02	1993		
4792 Lykaon	L5-An	10.0	59 d		40.09 ± 0.10	0.43 ± 0.02	1996	2	N
4805 Asteropaios	L5	9.9	62 d		12.372 ± 0.010	0.26 ± 0.01	1994	3	N
4827 Dares	L5-An	10.4	49 d		18.995 ± 0.028	0.24 ± 0.02	1994	3	N
4828 Misenus	L5-Mi	10.0	59 d		12.873 ± 0.016	0.33 ± 0.01	1995	3	N
4832 Palinurus	L5	9.8	65 d		5.319 ± 0.002	0.09 ± 0.02	2010	2	N
4833 Meges	L4	9.1	90 d	D	14.25 ± 0.03	0.13 ± 0.01	1995	3	N
4834 Thoas	L4	9.2	86 d		18.22 ± 0.04	0.14 ± 0.01	1996	3	N

Table 3
(Continued)

Asteroid	Trojan Cloud/ Family[a]	H	Estimated Diameter (km) and Source	Taxa	Syn. Period (hr)	Observed Amplitude	Apparition	Quality Code	Status
4836 Medon	L4	9.4	78 d		9.838 ± 0.008	0.24 ± 0.02	1991	3	N
					–	0.22 ± 0.02	1992		
					9.840 ± 0.013	0.31 ± 0.02	2009–2010		
4946 Askalaphus	L4-T	10.1	57 d		22.731 ± 0.018	0.40 ± 0.01	1992	3	N
5023 Agapenor	L4-WD	10.0	59 d		5.4020 ± 0.0017	0.12 ± 0.01	2009	2	N
5025 1986 TS_6	L4-M	10.3	52 d		∼253	∼0.2	2009	1	N
5027 Androgeos	L4	9.6	71 d		11.355 ± 0.013	0.31 ± 0.01	1992	3	N
5028 Halaesus	L4-T	9.9	62 d		24.937 ± 0.015	0.29 ± 0.01	1996	3	N
5119 1988 RA_1	L5-A	10.1	54 c		12.807 ± 0.016	0.31 ± 0.01	1994	3	N
5120 Bitias	L5-B	9.5	75 d		11.582 ± 0.017	⩾0.38	1993	2	N
5130 Ilioneus	L5-A	9.8	65 d		14.768 ± 0.014	0.16 ± 0.01	1994	3	N
5144 Achates	L5	8.9	94 c		5.949 ± 0.014	0.20 ± 0.01	1996	3	C
5254 Ulysses	L4	9.2	82 c		28.72 ± 0.08	0.32 ± 0.01	1996	3	N
5259 Epeigeus	L4	10.1	57 d		18.51 ± 0.03	0.10 ± 0.01	1995	3	N
5264 Telephus	L4	9.3	82 d	D	9.518 ± 0.013	0.34 ± 0.02	1994	3	N
5283 Pyrrhus	L4	9.3	82 c		–	0.04 ± 0.01	1996	3	N
					7.323 ± 0.003	0.11 ± 0.01	2002		
5476 1989 TO_{11}	L5	10.4	49 d		5.780 ± 0.001	0.30 ± 0.01	1994	3	N
5511 Cloanthus	L5-C	10.1	57 d		336 ± 7	⩾0.49	2010	1	N
5638 Deikoon	L5	10.0	59 d		9.137 ± 0.003	0.07 ± 0.01	1994	3	S
5648 1990 VU_1	L5	9.2	83 d		37.56 ± 0.05	0.20 ± 0.03	2009	3	S
6002 1988 RO	L5	10.4	49 d		12.918 ± 0.022	0.18 ± 0.01	1993	3	N
6090 1989 DJ	L4	9.4	78 d		18.60 ± 0.05	0.09 ± 0.01	1994	3	N
					18.476 ± 0.007	0.16 ± 0.01	2009		
7119 Hiera	L4-T	9.8	65 d		>400.	>0.10	2009	1	N
7641 1986 TT_6	L4	9.3	82 d		27.770 ± 0.013	0.40 ± 0.01	2009	3	N
9799 1996 RJ	L4	9.5	75 d		21.52 ± 0.03	0.16 ± 0.01	2009	3	N
11395 1998 XN_{77}	L4	9.5	75 d		13.70 ± 0.06	0.05 ± 0.01	2009	3	N
					13.696 ± 0.015	0.14 ± 0.01	2010		
11509 Thersilochos	L5-L	10.1	57 d		17.367 ± 0.015	0.27 ± 0.01	2010	3	N
12929 1999 TZ_1	L5	9.9	62 d		9.2749 ± 0.0016	0.17 ± 0.02	2009	3	S
16974 1998 WR_{21}	L4	9.8	65 d		78.9 ± 0.4	0.25 ± 0.01	2009	3	N
20729 1999 XS_{143}	L4	10.3	52 d		7.631 ± 0.006	0.13 ± 0.01	2009	3	S
21900 1999 VQ_{10}	L4-M	9.9	62 d		13.45 ± 0.08	0.18 ± 0.01	2009	2	N

Notes. [a] Collisional family membership according to Beauge & Roig (2001). Abbreviations are as follows: M: (1647) Menelaus; T: (2797) Teucer; WD: (4035) 1985 WD; P: (1869) Philoctetes; Ta: (3564) Talthybius; A: (1172) Aneas; B: (5120) Bitias; Mi: (4828) Misenus; An: (1173) Anchises; D: (1867) Deiphobus; Ph: (2357) Phereclos; Po: (4348) Poulydamas; C: (5511) Cloanthus; L: (6997) Laomedon.

1867 Deiphobus

Earlier observations by French (1987) suggested a rotation period longer than 24 hr. From seven nights in 1994 February we were able to pin the period of this slow rotator down to 58.66 ± 0.18 hr (see Figure 10). Although the period is firmly constrained, the determination of the light curve amplitude is more uncertain, as the shape of one maximum relies on the observations taken on February 9, which are not overlapping with any other.

1868 Thersites

Three nights in 1994 resulted in a reliable period of 10.4 hr, which is the first value published for this object (see Figure 11).

1873 Agenor

We observed this object during five nights in 1994 February (see Figure 12). The good accuracy and sampling of the measurements enabled us to determine an accurate rotation period notwithstanding the small amplitude and the comparatively long period.

2207 Antenor

Observations during the 1989 and 1996 apparitions show very irregular light curves, characterized by four maxima and four minima in 1989 (see Figure 13), and three maxima and three minima in 1996 (see Figure 14). In Gonano et al. (1991) we listed a preliminary determination of Antenor's rotation period and light curve amplitude based the 1989 observations, which are shown here for the first time. An earlier estimate of the light curve amplitude was published by Hartmann et al. (1988) from the data taken in 1983.

2223 Sarpedon

Observations from the 1994 and 1996 apparitions allowed us to derive a reliable rotation period of about 22.7 hr (see Figures 15 and 16). The near-commensurability with the duration of the Earth day required careful planning of the observations in order to achieve a complete coverage of the light curve. A lower bound for the amplitude, given by Hartmann et al. (1988) based on their unpublished observations of 1984, was the only previous literature information available for this object.

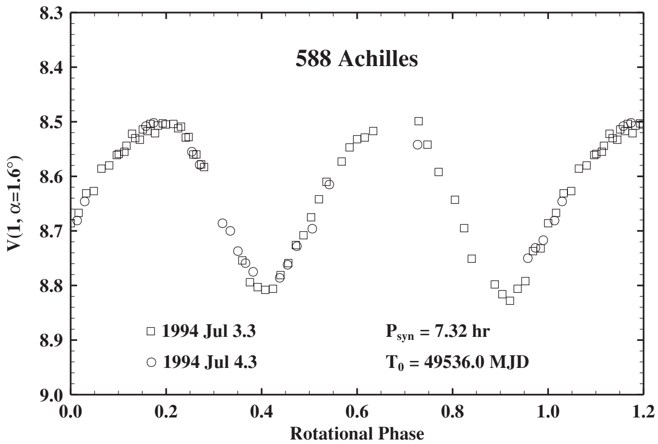

Figure 1. Composite light curve for 588 Achilles during the 1994 apparition.

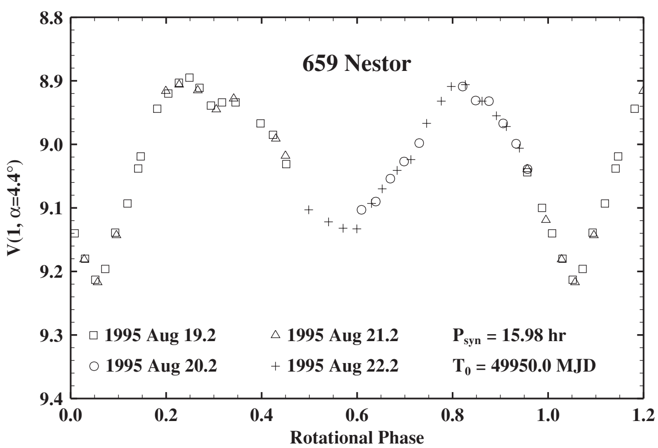

Figure 2. Composite light curve for 659 Nestor during the 1995 apparition.

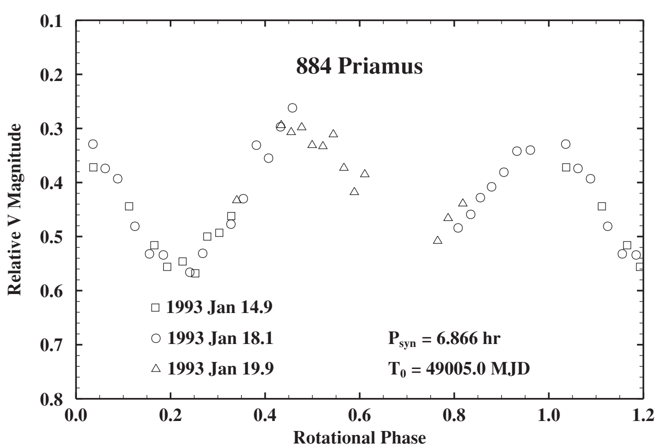

Figure 3. Composite light curve for 884 Priamus during the 1993 apparition.

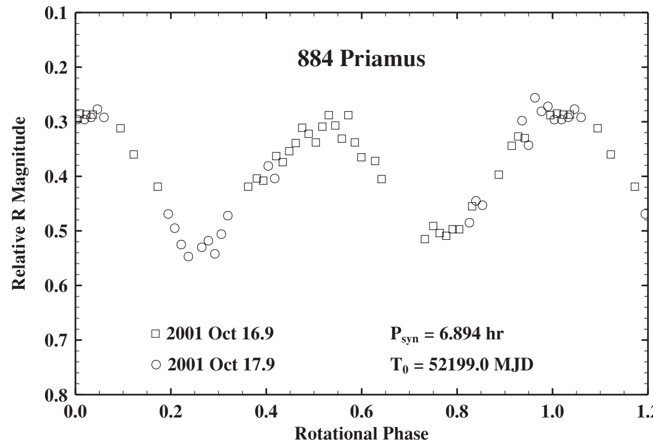

Figure 4. Composite light curve for 884 Priamus during the 2001 apparition.

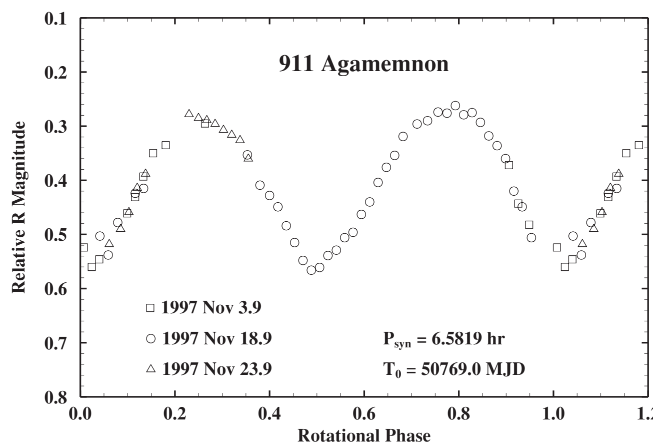

Figure 5. Composite light curve for 911 Agamemnon during the 1997 apparition.

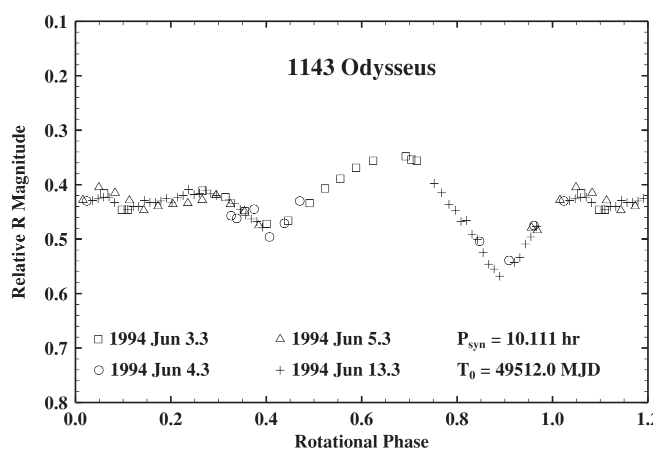

Figure 6. Composite light curve for 1143 Odysseus during the 1994 apparition.

2241 Alcathous

Observations from the 1991 apparition reveal a unique rotation period of about 7.7 hr (see Figure 17). An earlier estimation of 9.41 hr published by De Sanctis et al. (1994), based on six nights in 1992 December and 1993 January, corresponds to an alias of the correct period. Hartmann et al. (1988) reported an amplitude estimation for the 1994 apparition.

2260 Neoptolemus

From the apparitions of 1995 and 2002 we determined a unique rotation period of 8.18 hr (see Figures 18 and 19). Binzel & Sauter (1992) had guessed a period longer than 12 hr from their 1988 observations, while Angeli et al. (1999) suggested a period of 8.5 ± 0.1 hr, which, though outside their formal error, is closer to the correct period.

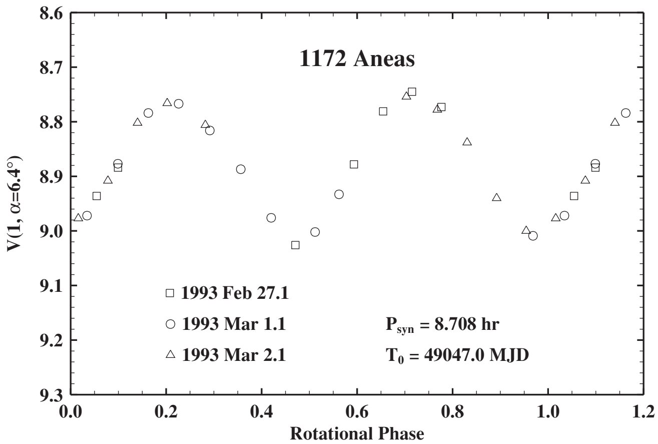

Figure 7. Composite light curve for 1172 Aneas during the 1993 apparition.

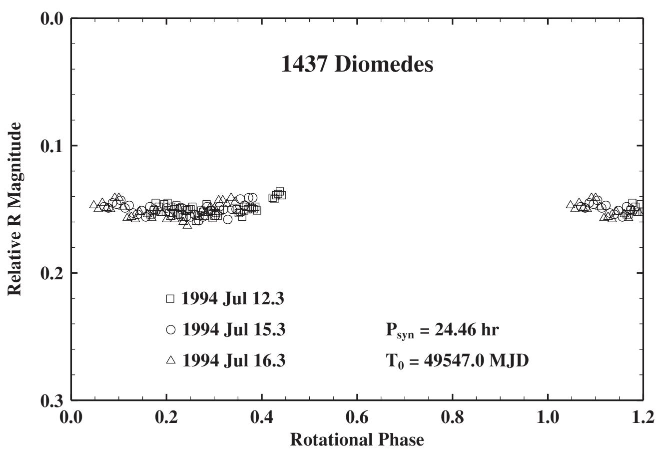

Figure 8. Composite light curve for 1437 Diomedes during the 1994 apparition.

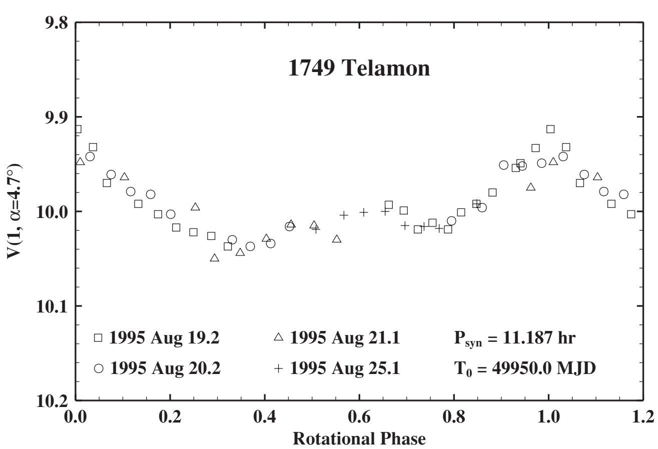

Figure 9. Composite light curve for 1749 Telamon during the 1995 apparition.

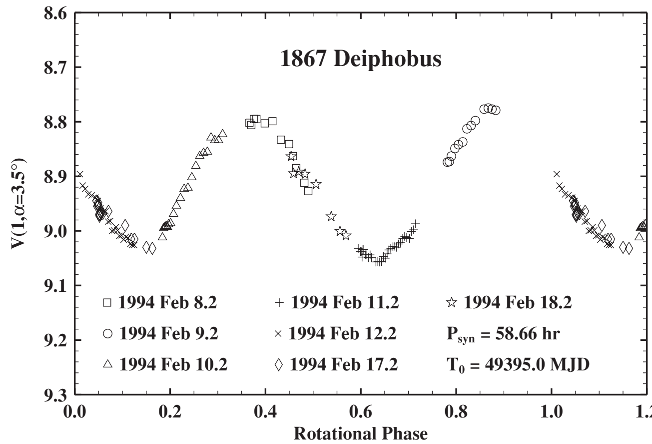

Figure 10. Composite light curve for 1867 Deiphobus during the 1994 apparition.

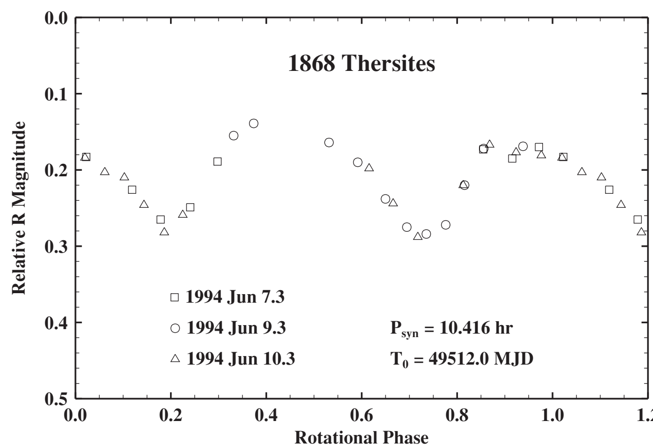

Figure 11. Composite light curve for 1868 Thersites during the 1994 apparition.

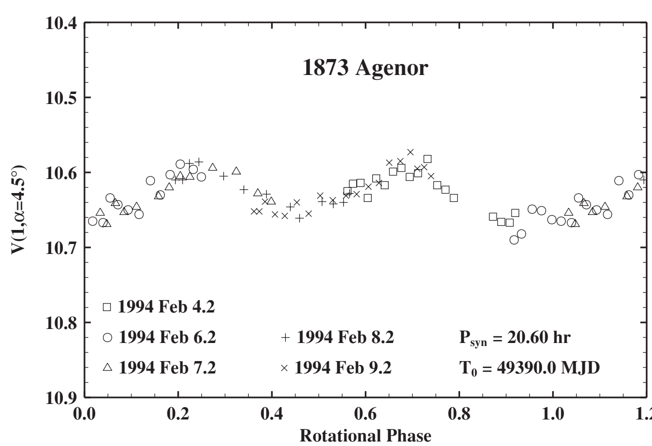

Figure 12. Composite light curve for 1873 Agenor during the 1994 apparition.

2357 Phereclos

Four nights of observations in 1994 revealed an irregular light curve with a low amplitude (see Figure 20), which made it difficult to estimate the number of cycles elapsed between subsequent nights, and resulted in multiple possible solutions. We observed this object again for seven nights in 2010, which enabled us to identify unambiguously a synodic period of about 14.4 hr (see Figure 21). Hartmann et al. (1988) report an amplitude of 0.14? [sic] for the 1987 apparition, possibly meaning that their determination is either noisy, or derived from an incomplete light curve coverage.

2363 Cebriones

Five nights of observations in 1994 resulted in a reliable rotation period of 20.05 hr for this object (see Figure 22). Galad & Kornos (2008) report a period of 20.081 hr from their measurements acquired during the 2008 apparition, which is compatible with our determination.

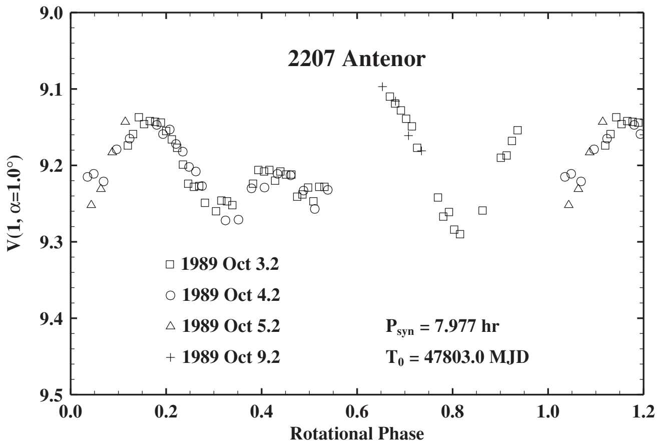

Figure 13. Composite light curve for 2207 Antenor during the 1989 apparition.

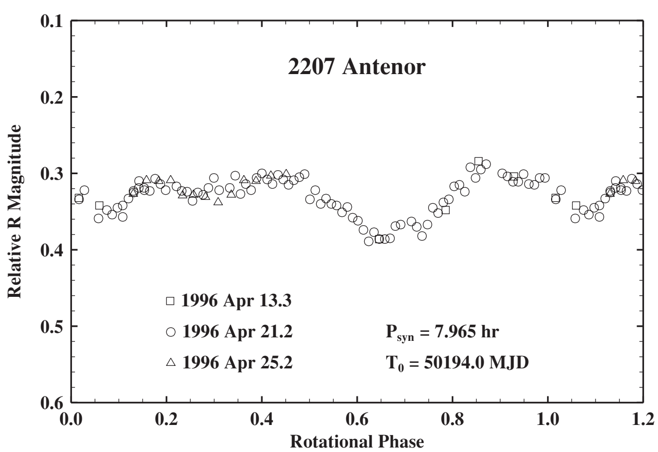

Figure 14. Composite light curve for 2207 Antenor during the 1996 apparition.

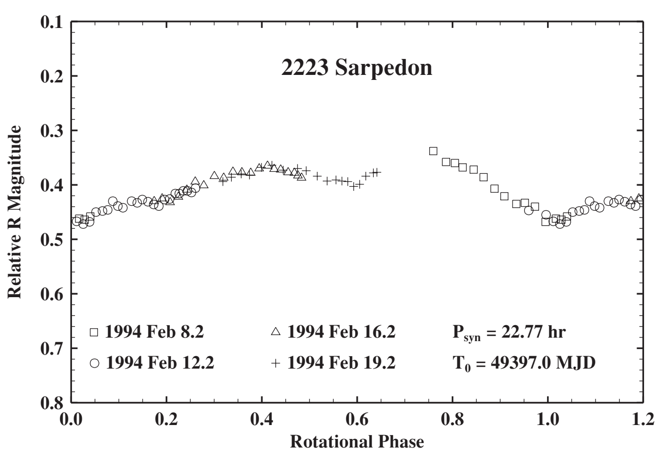

Figure 15. Composite light curve for 2223 Sarpedon during the 1994 apparition.

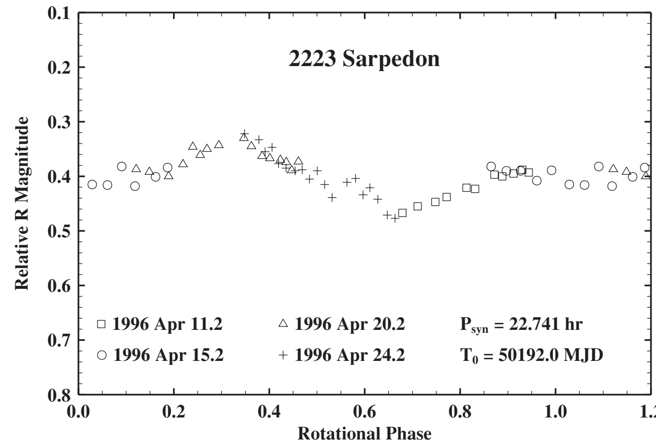

Figure 16. Composite light curve for 2223 Sarpedon during the 1996 apparition.

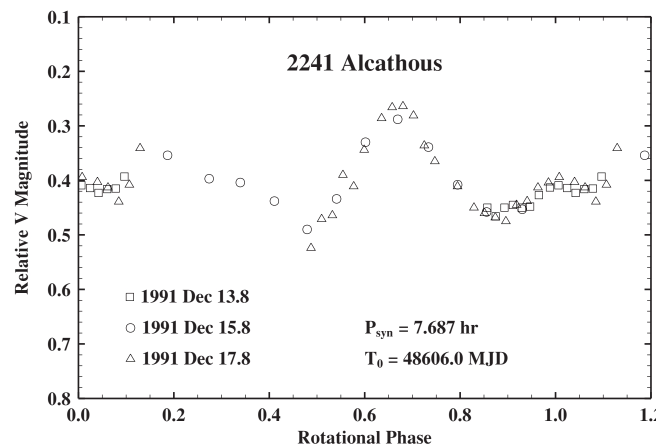

Figure 17. Composite light curve for 2241 Alcathous during the 1991 apparition.

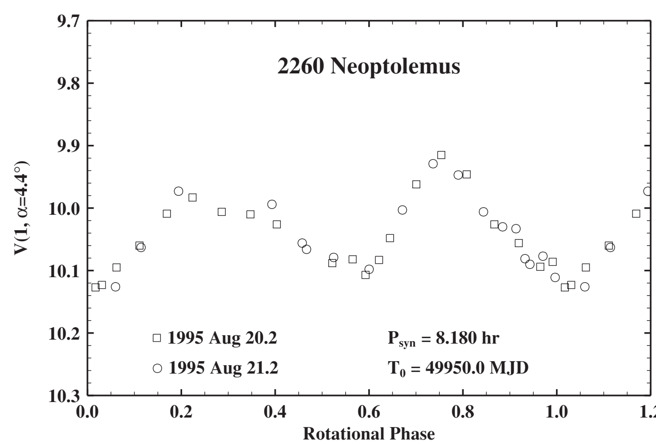

Figure 18. Composite light curve for 2260 Neoptolemus during the 1995 apparition.

2456 Palamedes

Our observations during four nights in 1995 June yield a synodic rotation period of 7.258 ± 0.004 hr, with an amplitude of only 0.05 mag (see Figure 23). Stephens (2010) published two nights of observations taken during the 2009 apparition, from which he determined a period of 7.24 ± 0.01 hr, which is in good agreement with our determination.

2674 Pandarus

French (1987) published a period of 8.4803 ± 0.0019 hr and a large light curve amplitude of 0.58 mag from three nights in 1986. Our observations spanning 8 hr with 105 data points from one night in 2001 October revealed virtually no light curve variation (see Figure 24), which implies a near polar view at the time of the observations. We used the French (1987) rotation period to plot our data versus rotational phase.

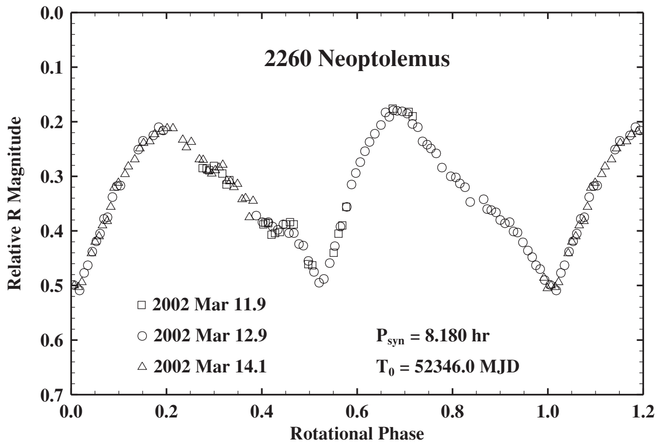

Figure 19. Composite light curve for 2260 Neoptolemus during the 2002 apparition.

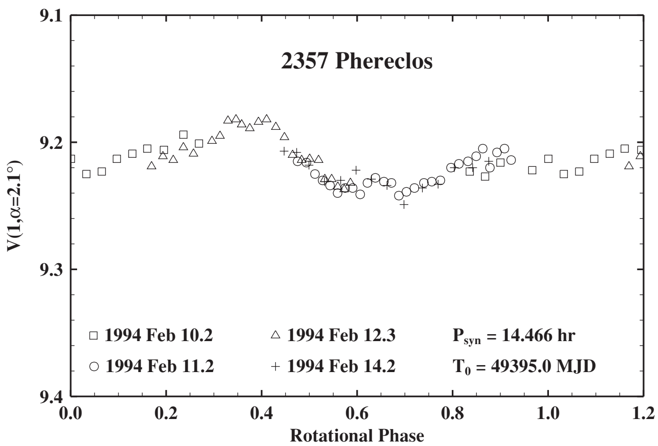

Figure 20. Composite light curve for 2357 Phereclos during the 1994 apparition.

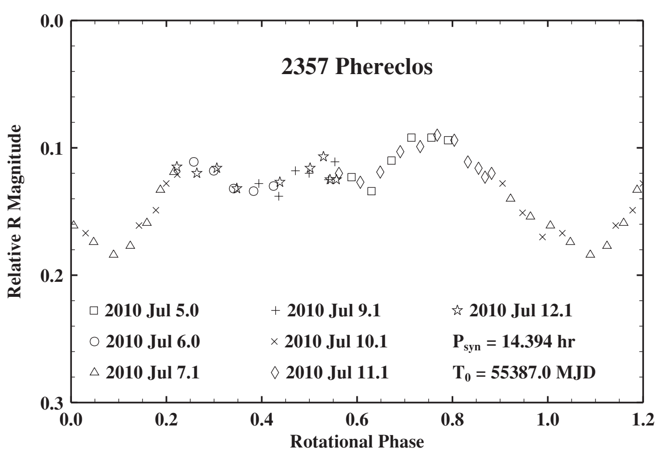

Figure 21. Composite light curve for 2357 Phereclos during the 2010 apparition.

2759 Idomeneus

Our first data of Idomeneus date back to the apparitions of 1991 and 1992, when we followed this object for a total of seven nights. The individual-night observations revealed a comparatively slow rotation. For this reason, the observations provided only an incomplete coverage of the rotation period and limited overlap among different nights. At that time, we searched for the rotation period that best fitted both sets of observations under the assumption of a double sine-wave light

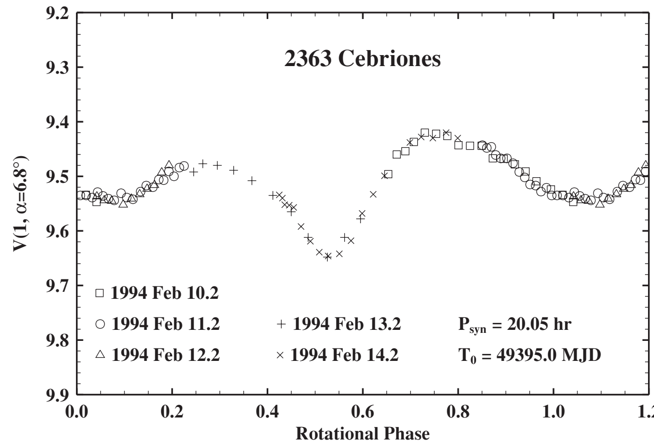

Figure 22. Composite light curve for 2363 Cebriones during the 1994 apparition.

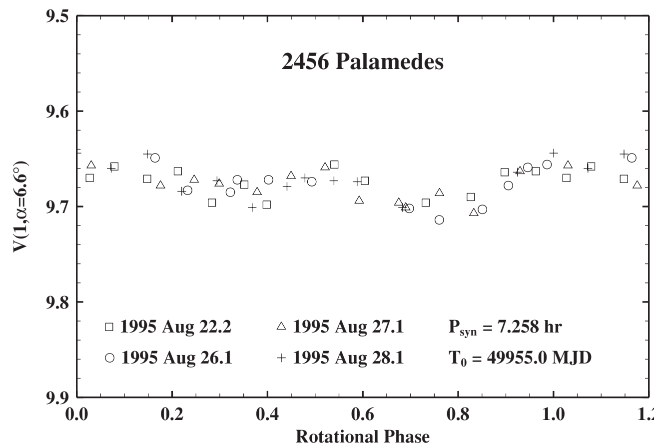

Figure 23. Composite light curve for 2456 Palamedes during the 1995 apparition.

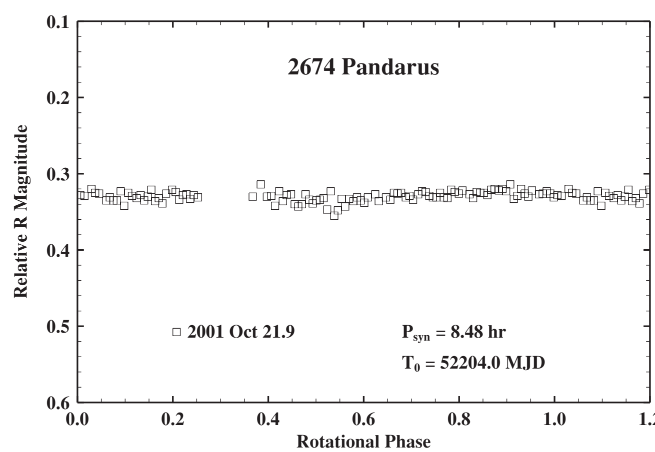

Figure 24. Composite light curve for 2674 Pandarus during the 2001 apparition.

curve, which resulted in a tentative value of about 32 hr. On 2010 December we had again the opportunity to observe Idomeneus, which allowed us to unambiguously confirm and refine its period to $P_{syn} = 32.38$ hr (see Figure 27). The observations of 1991 and 1992 are also folded with this period (see Figures 25 and 26).

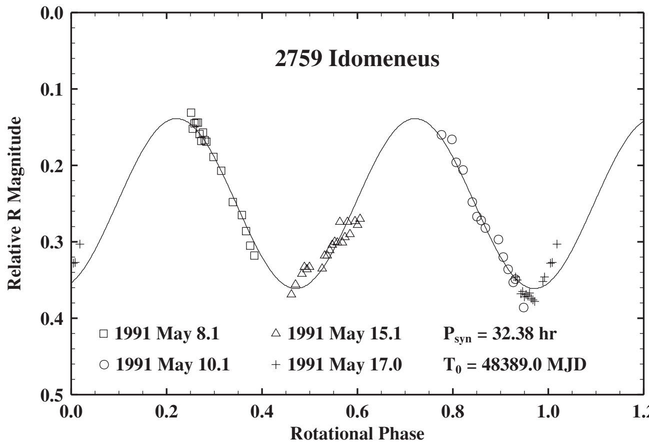

Figure 25. Composite light curve for 2759 Idomeneus during the 1991 apparition.

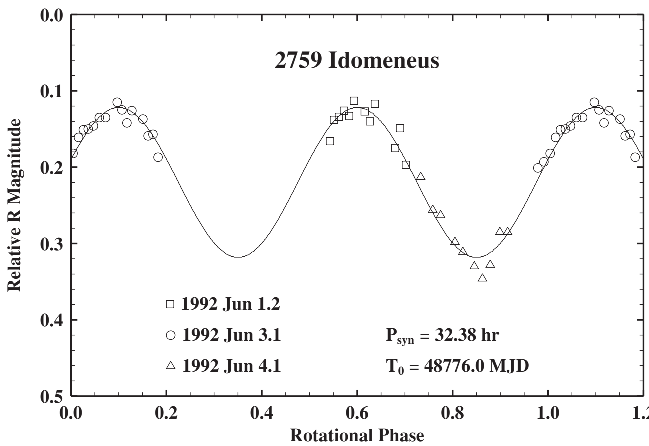

Figure 26. Composite light curve for 2759 Idomeneus during the 1992 apparition.

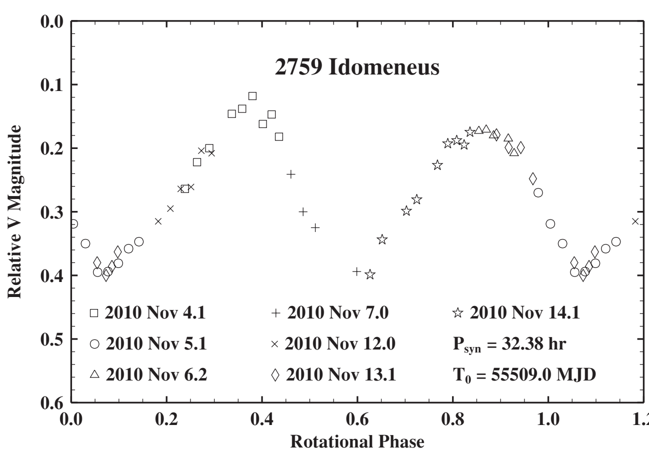

Figure 27. Composite light curve for 2759 Idomeneus during the 2010 apparition.

2895 Memnon

Our observations during three nights in 1990 November yield a reliable rotation period of 7.502 ± 0.010 hr (see Figure 28). Binzel & Sauter (1992) observed this object for 5 hr during a single night in 1990, from which they guessed a correct period of 7.5 hr.

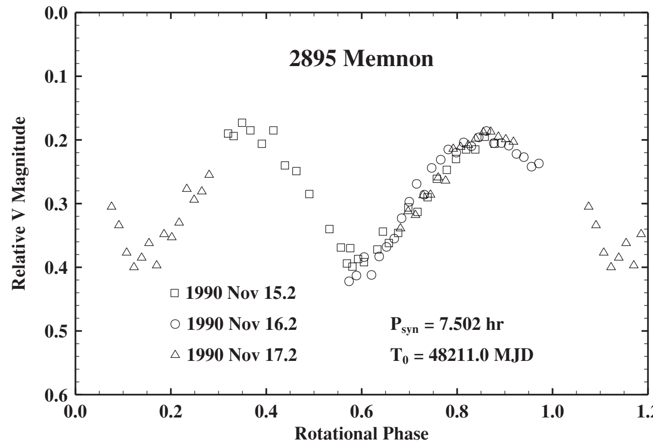

Figure 28. Composite light curve for 2895 Memnon during the 1990 apparition.

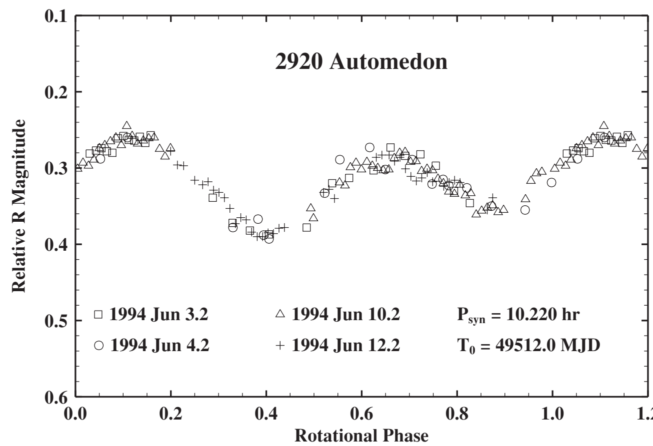

Figure 29. Composite light curve for 2920 Automedon during the 1994 apparition.

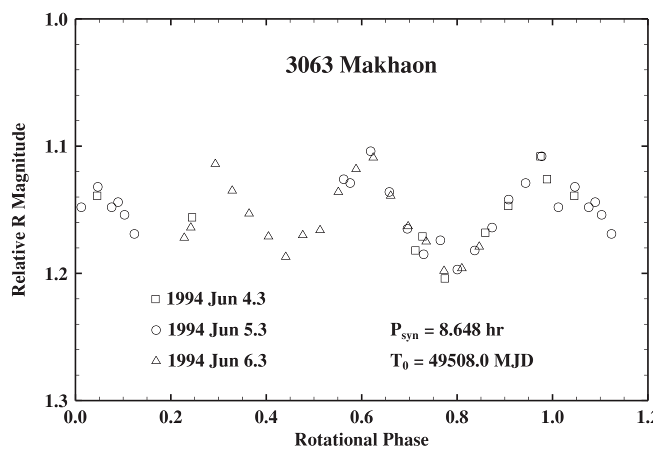

Figure 30. Composite light curve for 3063 Makhaon during the 1994 apparition.

2920 Automedon

Four nights of observations in 1994 allowed us to determine an unambiguous rotation period of 10.220 ± 0.004 hr (see Figure 29), which is in excellent agreement with the determination by Molnar et al. (2008).

3063 Makhaon

We observed 3063 Makhaon in two apparitions, during which the asteroid displayed a small light curve amplitude. As it often

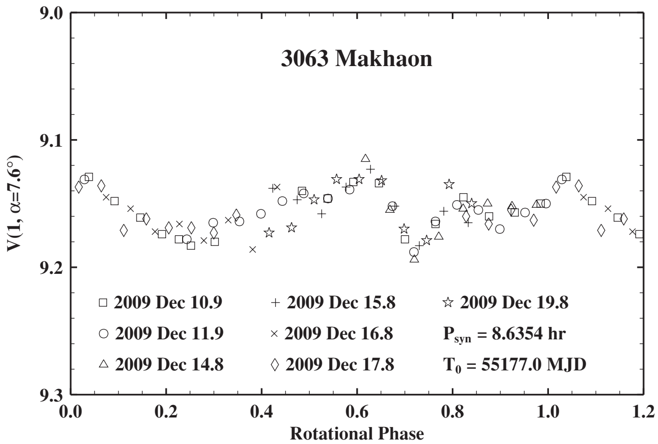

Figure 31. Composite light curve for 3063 Makhaon during the 2009 apparition.

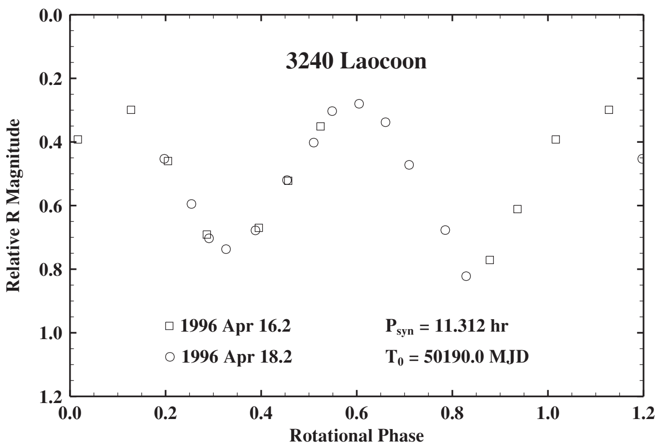

Figure 32. Composite light curve for 3240 Laocoon during the 1996 apparition.

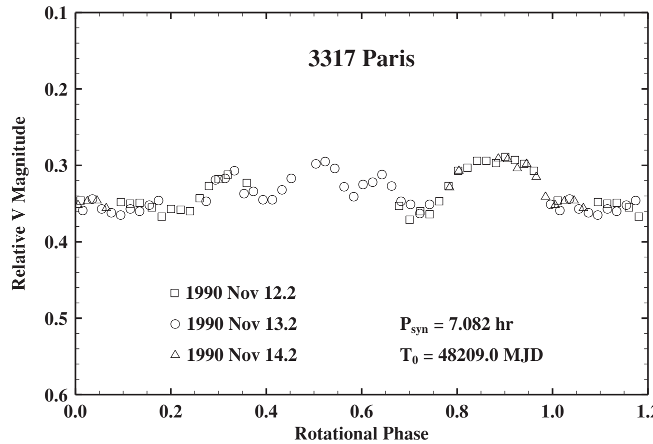

Figure 33. Composite light curve for 3317 Paris during the 1990 apparition.

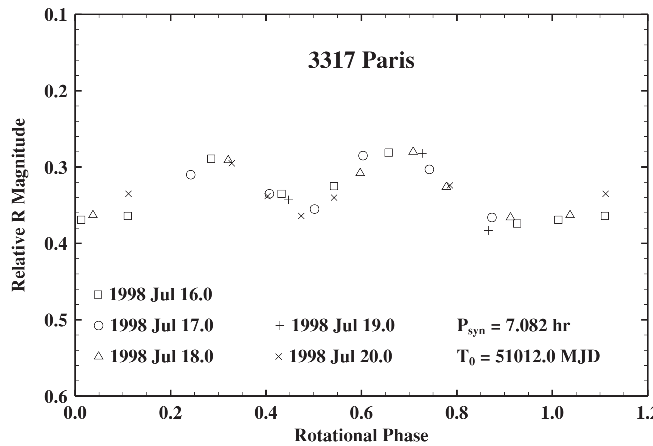

Figure 34. Composite light curve for 3317 Paris during the 1998 apparition.

happens in these cases, the light curve was very irregular, with multiple maxima and minima. We found a unique solution that best fits both apparitions with a rotation period of about 8.6 hr (see Figures 30 and 31). The resulting rotation coverage is complete and the reproducibility of the measurements on subsequent nights is good.

This object was also observed by Binzel & Sauter (1992) in 1988, who collected light curves during two consecutive nights of observations. Based on these data, the authors suggested a period of 17.3 hr, under the assumption of a two-maximum two-minimum light curve. We have composited the data by Binzel & Sauter with our period and we obtained an excellent fit. At the time of their observations, 3063 was characterized by a prominent maximum–minimum feature, and displayed only a hint of a secondary maximum and minimum, which led the authors to derive a period double as long as the real one.

3240 Laocoon

We observed this object during two nights in 1996 April from which a reliable period of 11.312 ± 0.014 hr could be determined (see Figure 32). For this object only an amplitude estimate was previously available (Hartmann et al. 1988).

3317 Paris

We observed Paris during three nights in 1990 November when the object displayed a low amplitude and a very irregular shape (see Figure 33). The anomalous number of maxima and minima made it difficult at that time to estimate the fundamental periodicity. For this reason, we observed the object again for five nights in 1998, from which we could determine an unambiguous synodic period of 7.082 ± 0.003 hr (see Figure 34). Behrend (2010) reports on his Web page independent observations by René Roy and by Federico Manzini, who derive a rotation period compatible with our determination.

3451 Mentor

We observed this object during the apparitions of 1993 and 1998, from which we derived a period of 7.7 hr (see Figures 35 and 36). A series of earlier period determinations, all compatible with our value, have been published (Sauppe et al. 2007; Duffard et al. 2008; Melita et al. 2010). In addition, light curves by several authors have been published online by Behrend (2010). An amplitude estimate from observations in 1987 can be found in Hartmann et al. (1988).

3548 Eurybates

We observed this object during the 1992 apparition for four nights and derived an unambiguous rotation period of 8.711 hr (see Figure 37). Stephens (2010) reports his own observations of 3548 Eurybates during two nights in the 2009 opposition that enabled him to independently determine a rotation period of 8.73 hr. The two determinations are in excellent agreement, within the respective uncertainties.

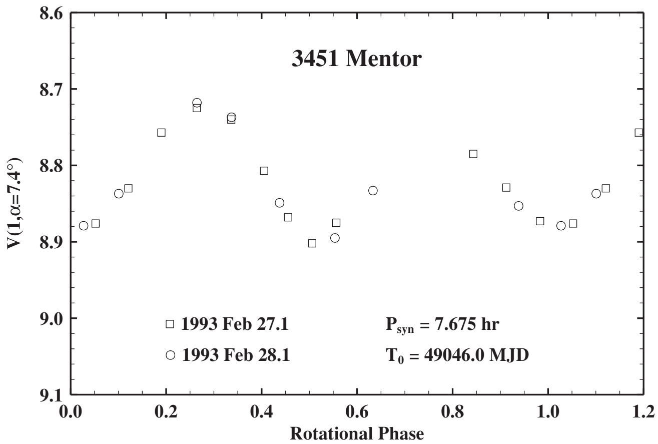

Figure 35. Composite light curve for 3451 Mentor during the 1993 apparition.

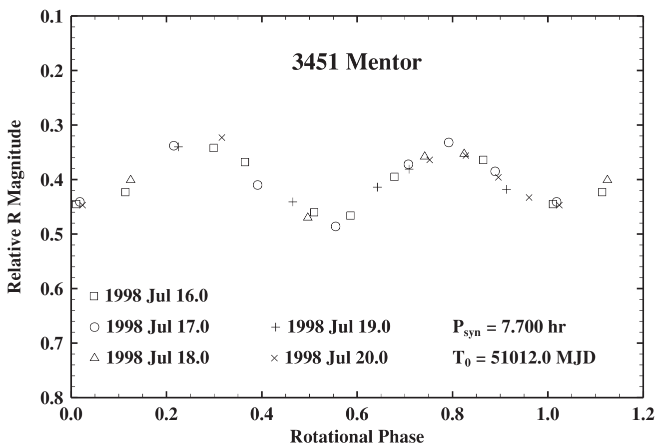

Figure 36. Composite light curve for 3451 Mentor during the 1998 apparition.

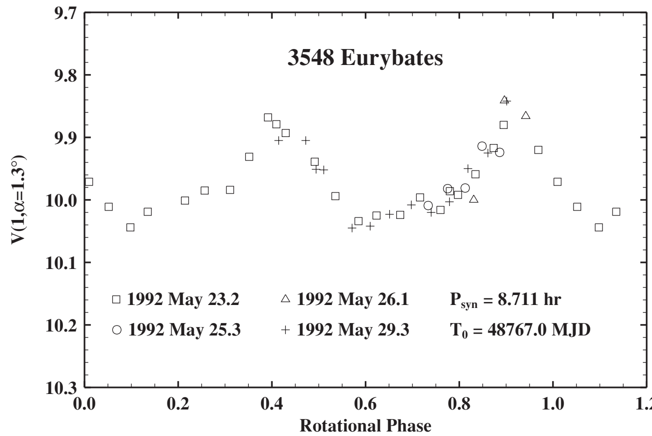

Figure 37. Composite light curve for 3548 Eurybates during the 1992 apparition.

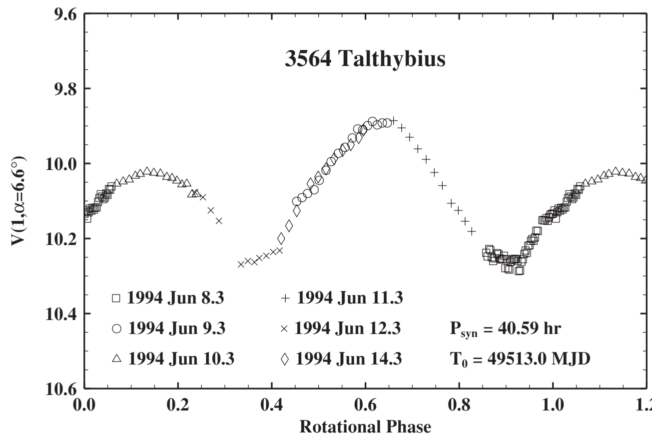

Figure 38. Composite light curve for 3564 Talthybius during the 1994 apparition.

At the time of Stephens' observations, the asteroid was located at an ecliptic longitude almost exactly 180° apart from that during our observations. This coincidence resulted in very similar viewing conditions, and consequently, similar light curve shapes and amplitudes.

3564 Talthybius

Six nights of observations in 1994 June resulted in a composite with a complete coverage for this comparatively slow rotator (see Figure 38). The unambiguous period of 40.59 ± 0.13 hr is in agreement with the recent determination by Stephens (2010).

3708 1974 FV_1

Three nights of observations in 1993 resulted in an unambiguous period of 6.55 hr (see Figure 39). No previous period determinations have been published for this object.

3793 Leonteus

In 1994, this object displayed a regular two-maximum two-minimum light curve with a period of 5.62 hr and an amplitude of 0.24 mag (see Figure 40). In 1997, the object had a much smaller amplitude and a single maximum–minimum light curve (see Figure 41). Stephens (2010) reports his observations of 2009, during which the viewing geometry was very close to that of 1997. For this reason the one-maximum one-minimum appearance of the light curve led Stephens to estimate a wrong rotation period of 11.22 hr.

3794 Sthenelos

Four nights of observations in 1995 August allowed us to determine the rotation period of this object (see Figure 42). Quick-look data reduction at the telescope allowed us to schedule the observations to cover the whole period, despite the near 2:1 commensurability with the length of the Earth day.

4007 Euryalos

We observed Euryalos in 1995 for four nights (see Figure 43). Despite the low amplitude displayed during that apparition, we could determine a reliable rotation period, which constitutes the first determination published for this object.

4035 1986 WD

We observed this object for the first time during two nights in 1991 May (see Figure 44). From these observations alone, however, an unambiguous rotation period could not be derived, due to the difficulty in the estimation of the elapsed cycles between the observations. In 2009, we had a second opportunity to observe 1986 WD, which finally resulted in a solid determination of 13.467 hr (see Figure 45). The object displays a peculiar light curve, with a bilobated secondary maximum. By chance, during the observations of 1991 and 2009 the object was visible from Earth from almost exactly opposite directions. For this reason, the shape of the light curve during the two apparitions is very

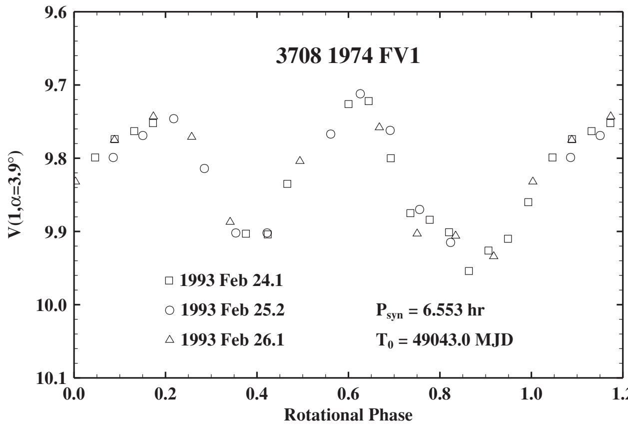

Figure 39. Composite light curve for 3708 1974 FV_1 during the 1993 apparition.

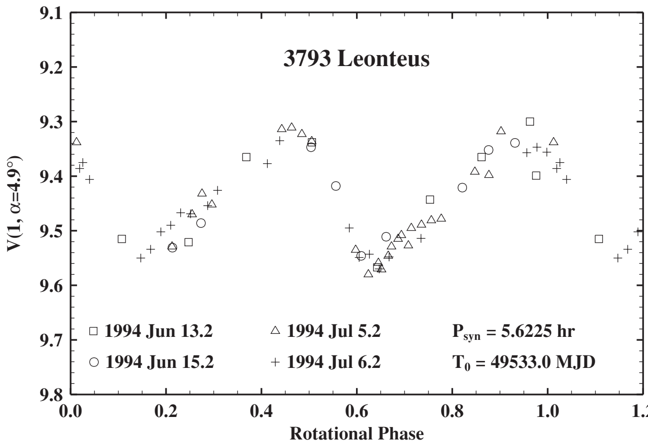

Figure 40. Composite light curve for 3793 Leonteus during the 1994 apparition.

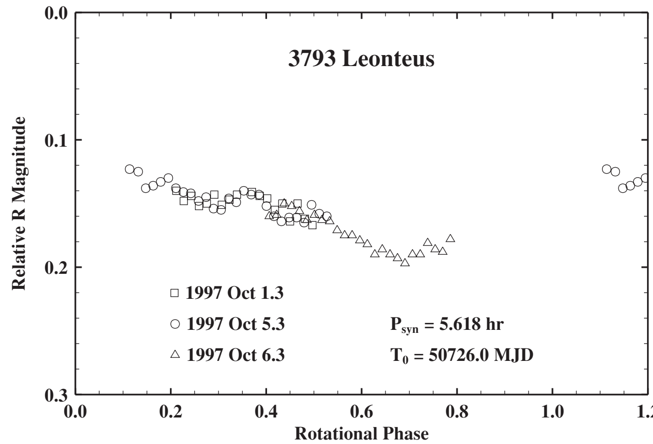

Figure 41. Composite light curve for 3793 Leonteus during the 1997 apparition.

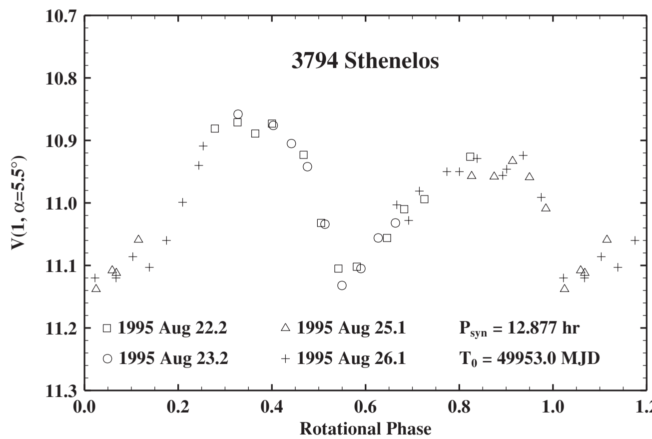

Figure 42. Composite light curve for 3794 Sthenelos during the 1995 apparition.

similar. No previous period determinations are available in the literature for this object.

4057 Demophon

We derive a period of 29.31 ± 0.07 hr from six nights of observations in 1994 (see Figure 46). The only previous published determination for this object is an amplitude estimation for the 1986 apparition by Hartmann et al. (1988).

4063 Euforbo

From two consecutive nights in 1992, showing two maxima and one minimum, and one maximum and two minima, respectively, we could determine a reliable period for Euforbo, which constitutes its first period determination published (see Figure 47).

4086 Podalirius

We observed Podalirius on three consecutive nights in 1991 May, from which we derived a best-fit period of 10.43 hr (see Figure 48). Stephens (2009) reports his observations of this object during two consecutive nights in 2008 October, and on a third night one week later. From these data he derives a period of 14.51 hr, which corresponds approximately to a 3.5:5 alias of our period. We plotted R. D. Stephens' original data (2009, private communication) with our own period of 10.43 hr, and actually obtained a better solution than that published in the original reference. With our period, Stephens' composite displays only one maximum and one minimum, and perhaps for this reason, the author had rejected the correct solution.

4348 Poulydamas

Three nights of observations in 1990 resulted in an unambiguous rotation period of about 9.9 hr (see Figure 49). No other determinations have been previously published for this object.

4489 1988 AK

Four consecutive nights of observations in 1995 August revealed a light curve with an extremely low amplitude and an irregular shape. The Fourier analysis produced two possible periods around 16.2 hr and 12.6 hr, with the former having a slightly higher significance. Because of the very low amplitude, however, combined with the uncertainty about the number of maxima and minima, a certain period determination was not possible. For this reason, we re-observed this object for 10 nights during the 2010 apparition, when, due to a different viewing geometry, the object happened to display a larger amplitude. These latter observations (see Figure 51) allowed us to determine an unambiguous period of 12.582 hr, which represents the first published value for this object. This period was also used to

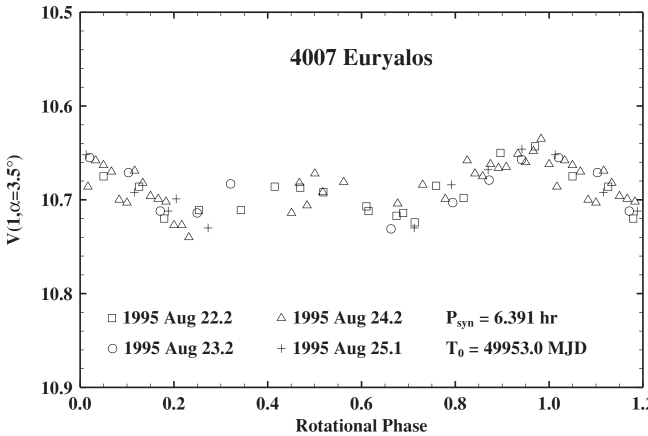

Figure 43. Composite light curve for 4007 Euryalos during the 1995 apparition.

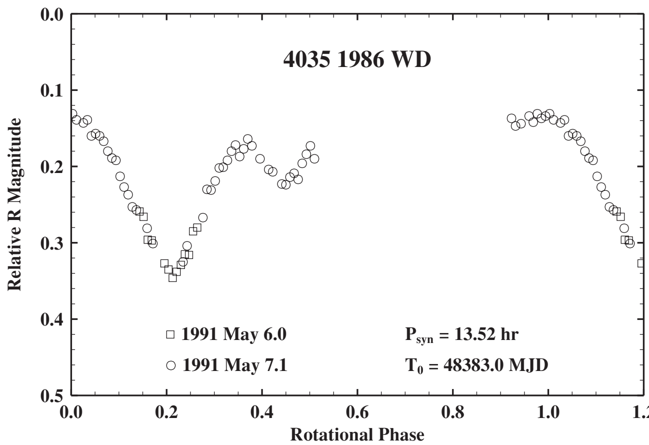

Figure 44. Composite light curve for 4035 1986 WD during the 1991 apparition.

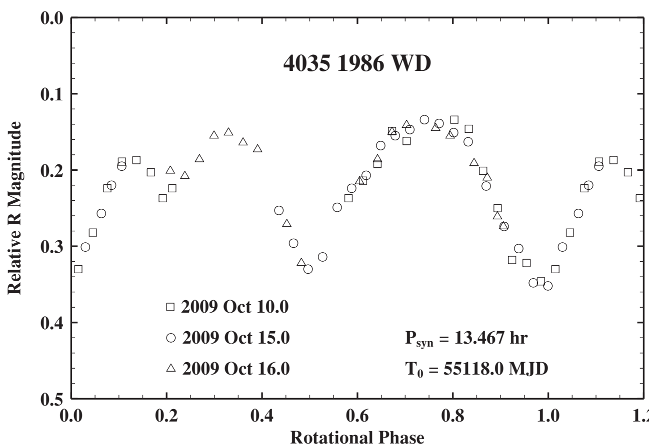

Figure 45. Composite light curve for 4035 1986 WD during the 2009 apparition.

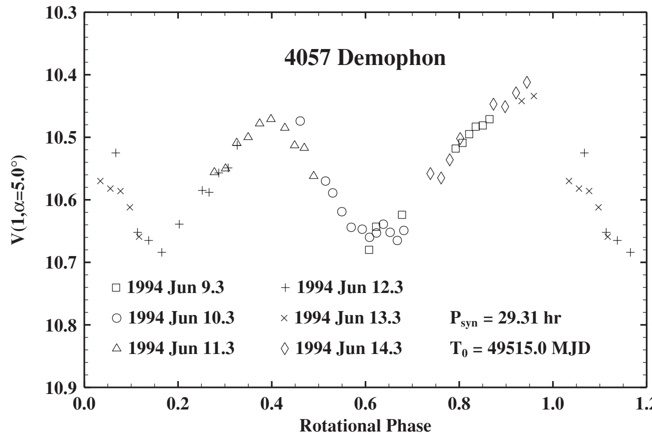

Figure 46. Composite light curve for 4057 Demophon during the 1994 apparition.

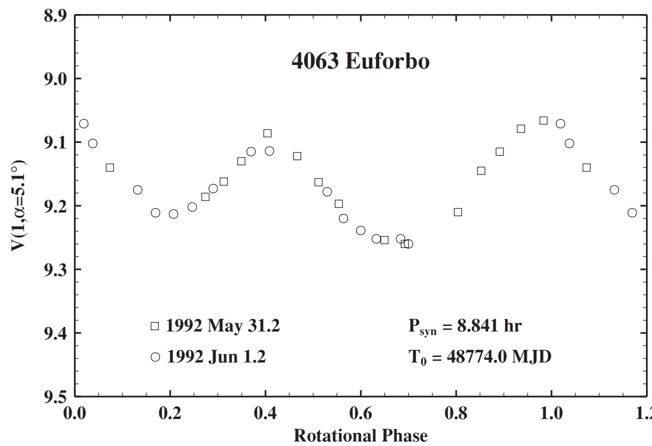

Figure 47. Composite light curve for 4063 Euforbo during the 1992 apparition.

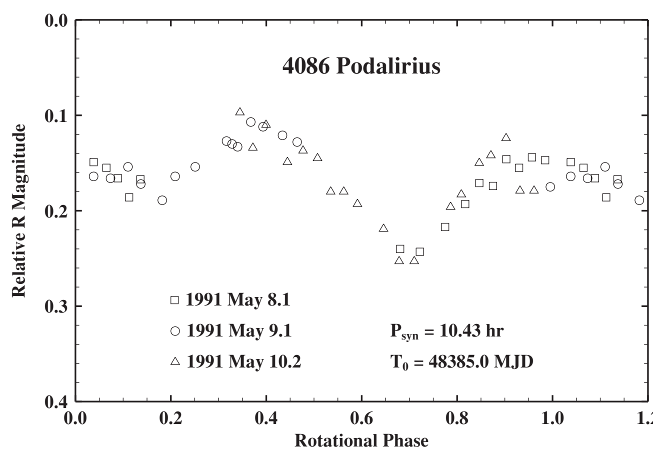

Figure 48. Composite light curve for 4086 Podalirius during the 1991 apparition.

produce the composite for the 1995 observations (see Figure 50), during which the object must have shown us a near polar view.

4543 Phoinix

This object was observed from two stations for a total of 12 nights over a time span of about seven weeks during the winter of 2009 (see Figure 52). Even though due to the long rotation period and to bad weather we covered only about 74% of the light curve, the derived period solution is unique. This is partly due to the fact that, whenever possible, we made use of the same set of comparison field stars on consecutive nights, which, by reducing the number of parameters fitted, makes the solution more stable, especially for long rotation periods.

4709 Ennomos

Five nights of observations in 1990 enabled us to determine an unambiguous rotational period for this object (see Figure 53). Because the period is close to 12 hr, near real-time data reduction

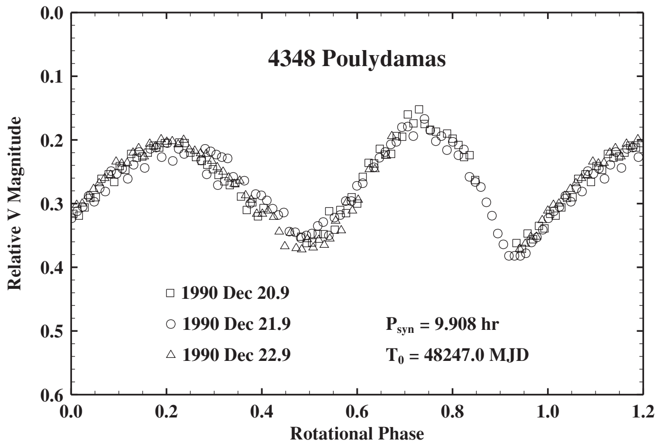

Figure 49. Composite light curve for 4348 Poulydamas during the 1990 apparition.

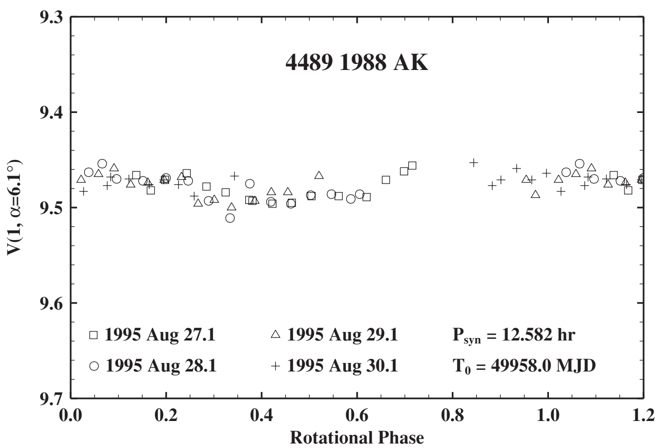

Figure 50. Composite light curve for 4489 1988 AK during the 1995 apparition.

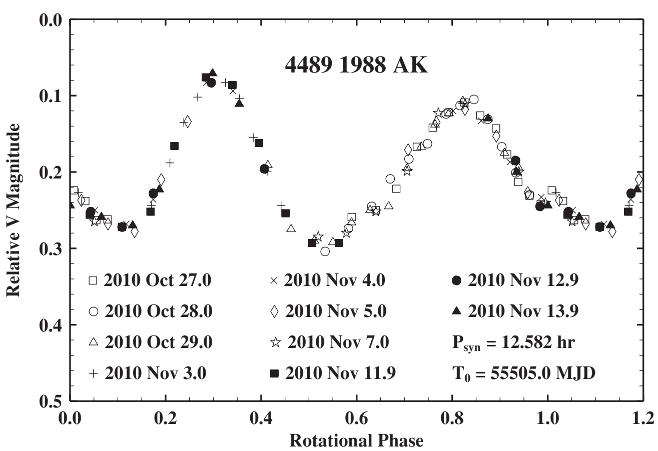

Figure 51. Composite light curve for 4489 1988 AK during the 2010 apparition.

was key to planning the following nights' observations, which helped us achieve a complete rotational coverage.

4715 1989 TS_1

We observed this object during four nights in 1991 and unambiguously determined its rotation period (see Figure 54), which represents the first value published for this object.

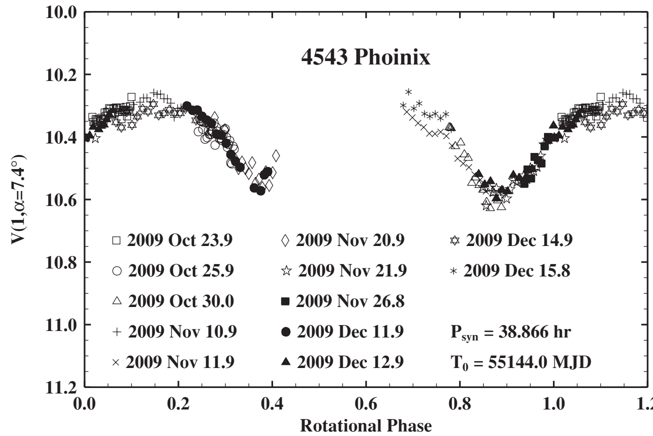

Figure 52. Composite light curve for 4543 Phoinix during the 2009 apparition.

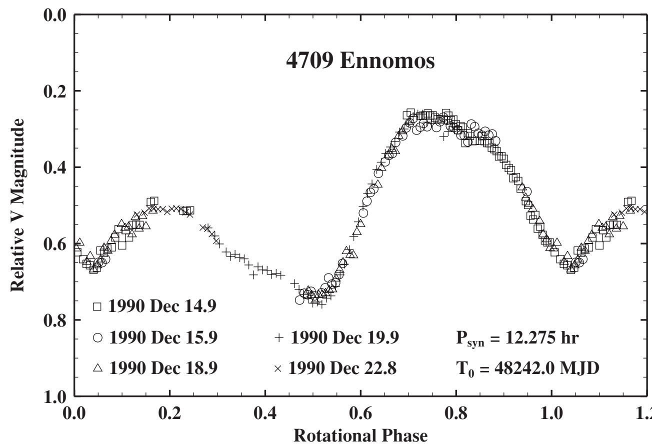

Figure 53. Composite light curve for 4709 Ennomos during the 1990 apparition.

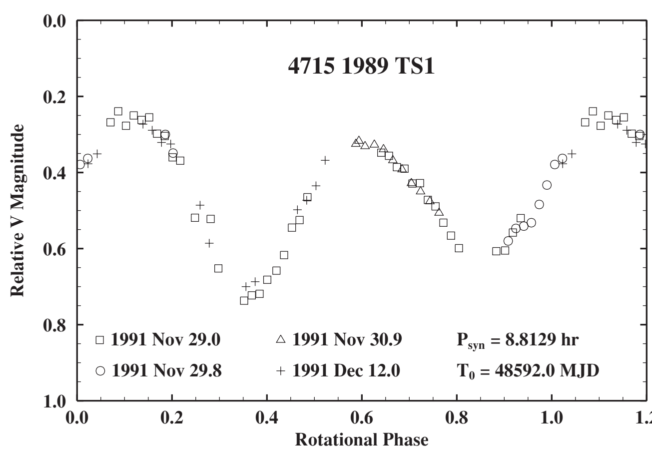

Figure 54. Composite light curve for 4715 1989 TS_1 during the 1991 apparition.

4722 Agelaos

From observations on two consecutive nights in 2002 December we determined a rotation period of about 18.6 hr. Although the composite covers only about 75% of the complete period (see Figure 55), and there is no overlap between the two nights, the solution is unique. During the two nights, the same set of in-field comparison stars was observed, so that no arbitrary magnitude shift was applied to compile the composite. No previous determinations have been published for this object.

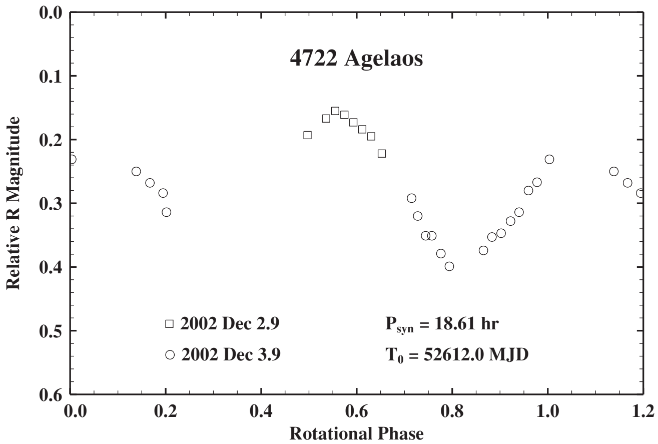

Figure 55. Composite light curve for 4722 Agelaos during the 2002 apparition.

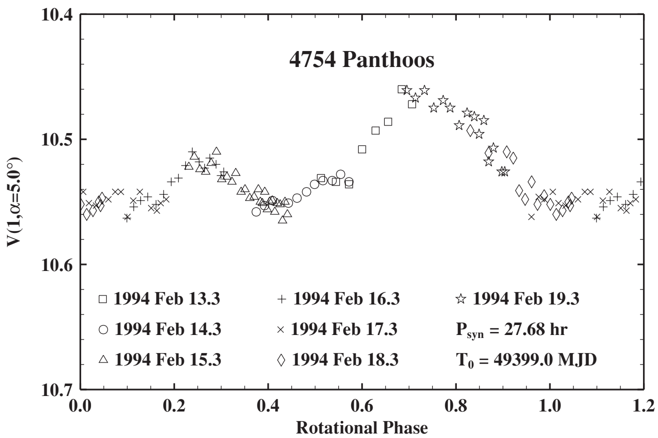

Figure 56. Composite light curve for 4754 Panthoos during the 1994 apparition.

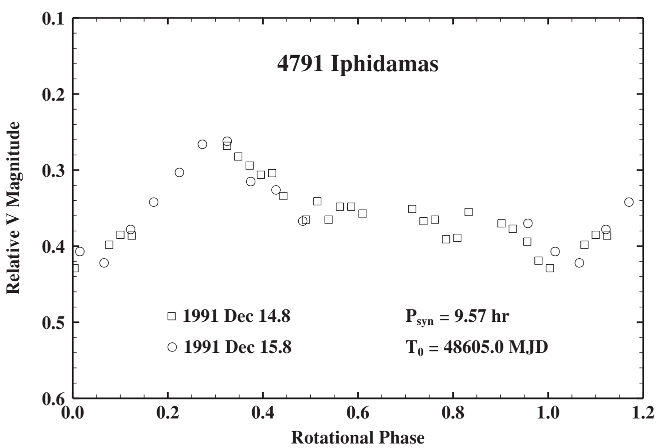

Figure 57. Composite light curve for 4791 Iphidamas during the 1991 apparition.

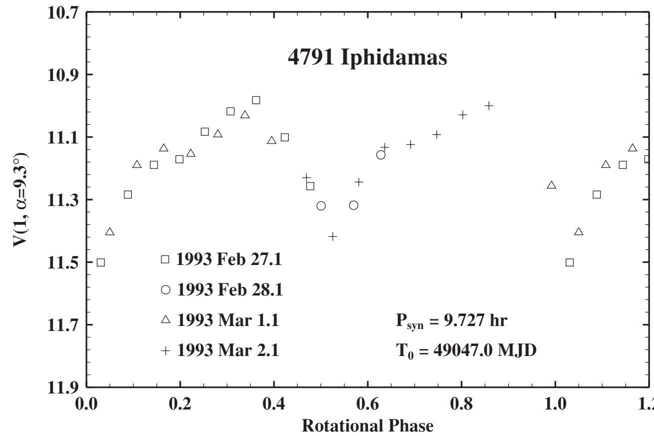

Figure 58. Composite light curve for 4791 Iphidamas during the 1993 apparition.

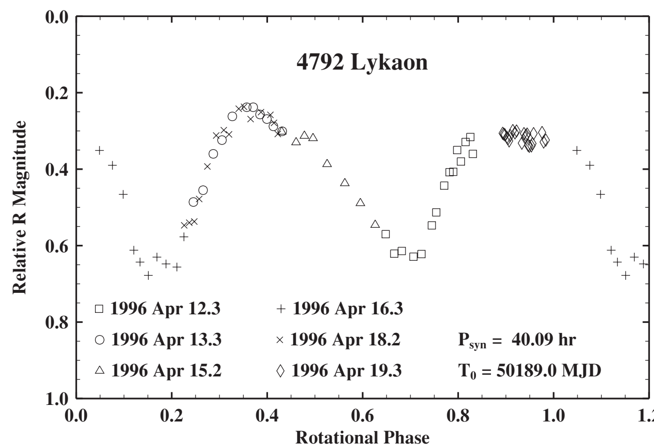

Figure 59. Composite light curve for 4792 Lykaon during the 1996 apparition.

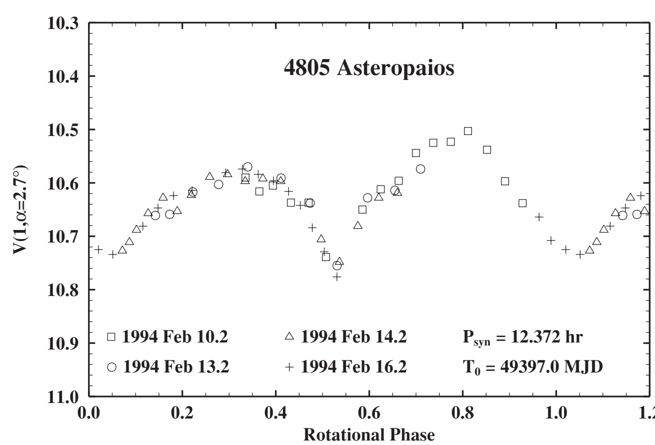

Figure 60. Composite light curve for 4805 Asteropaios during the 1994 apparition.

4754 Panthoos

Seven consecutive nights of observations in 1994 February enabled us to determine and completely cover the rotation period of this comparatively slow rotator (see Figure 56). This is the first determination published for this object.

4791 Iphidamas

From two runs, in 1991 and 1993, we could determine an unambiguous rotation period of about 9.73 hr. During the 1991 apparition, the object displayed only one maximum and one minimum in its light curve (see Figure 57), while in 1993 it showed two pairs of extrema (see Figure 58).

4792 Lykaon

A total of six nights of observations allowed us to determine a rotation period of about 40 hr for this object, under the assumption of two maxima and two minima per rotation cycle (see Figure 59). The observations taken during the night of

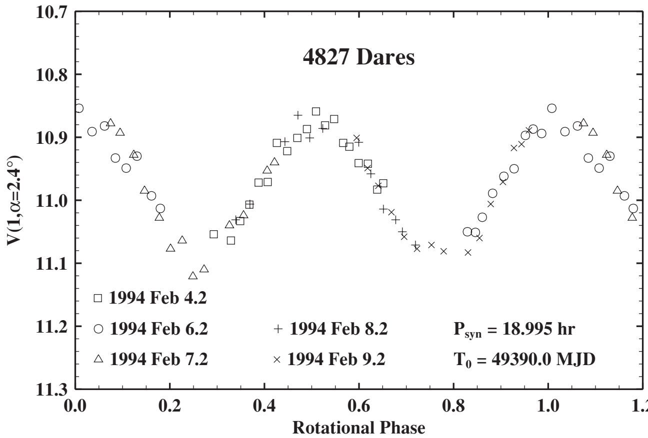

Figure 61. Composite light curve for 4827 Dares during the 1994 apparition.

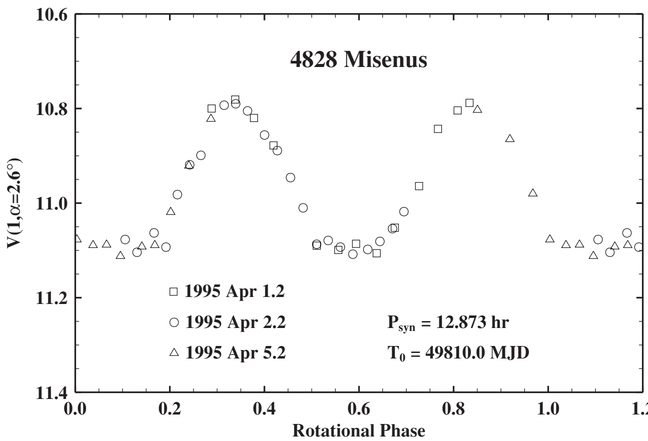

Figure 62. Composite light curve for 4828 Misenus during the 1995 apparition.

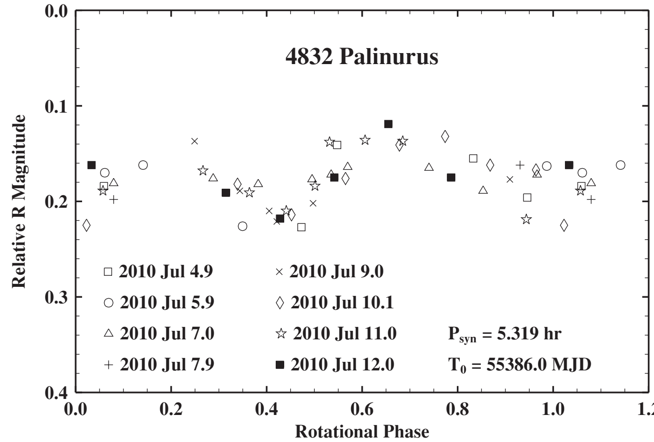

Figure 63. Composite light curve for 4832 Palinurus during the 2010 apparition.

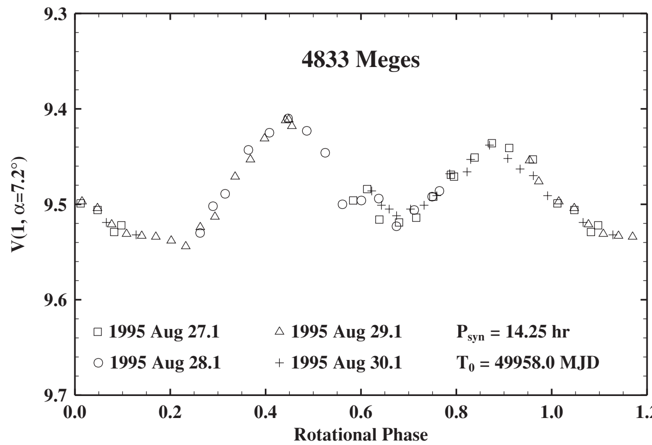

Figure 64. Composite light curve for 4833 Meges during the 1995 apparition.

1996 April 19, which cover the secondary maximum of the light curve, do not overlap with observations from any other nights. For this reason, the amplitude of the secondary maximum is not well constrained. No previous photometric measurements are reported in the literature for this object.

4805 Asteropaios

Four nights of observations in 1994 February provided full coverage of the rotational cycle of this object, enabling us to determine an unambiguous period of about 12.4 hr (see Figure 60). This represents the first determination published for Asteropaios.

4827 Dares

Five nights of observations resulted in multiple coverage of the rotation period of nearly 19 hr (see Figure 61), which represents the first determination published for Dares.

4828 Misenus

We observed Misenus for three nights in 1995. From a well-sampled light curve we could determine an unambiguous period of about 12.9 hr (see Figure 62), which represents the first estimate published for this object.

4832 Palinurus

We observed this object during eight consecutive nights of observations in 2010 (see Figure 63). However, due to the comparatively low amplitude of the light curve, and to the rather noisy data set due to the object being located in a crowded field, it was difficult to estimate the number of cycles elapsed per night. Therefore, the resulting best-fit period of about 5.3 hr should be regarded as tentative.

4833 Meges

Four nights in 1995 August resulted in a reliable period of 14.25 hr (see Figure 64). No other photometric measurements have been published for this object to date.

4834 Thoas

During four nights of observations in 1996 September the object displayed an asymmetric light curve with a subdued secondary minimum (see Figure 65). An unambiguous period of about 18.2 hr represents the first determination published for this object.

4836 Medon

We observed this object for the first time during its 1991 apparition. The asteroid displayed an irregular light curve with the presence of additional maxima and minima (see Figure 66), which made it difficult to estimate the fundamental periodicity. Two solutions were equally likely. In order to resolve this ambiguity we re-observed this object during two more apparitions, that of 1992 (see Figure 67) and of 2009–2010

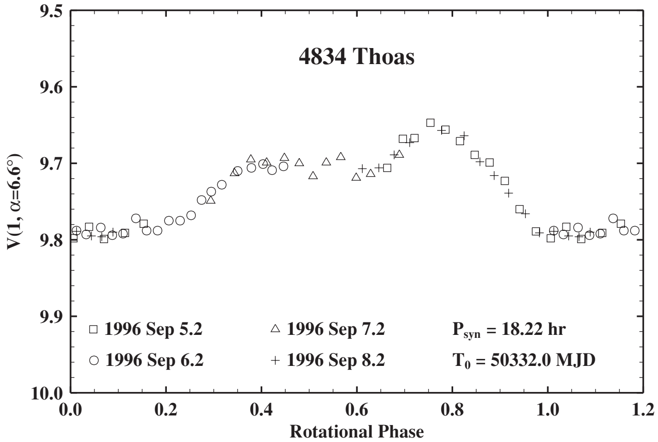

Figure 65. Composite light curve for 4834 Thoas during the 1996 apparition.

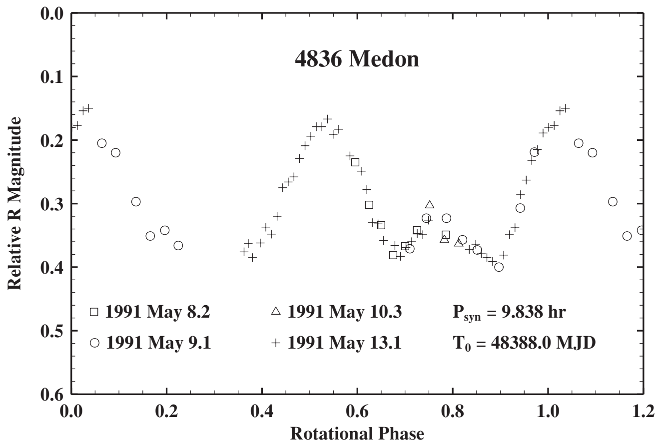

Figure 66. Composite light curve for 4836 Medon during the 1991 apparition.

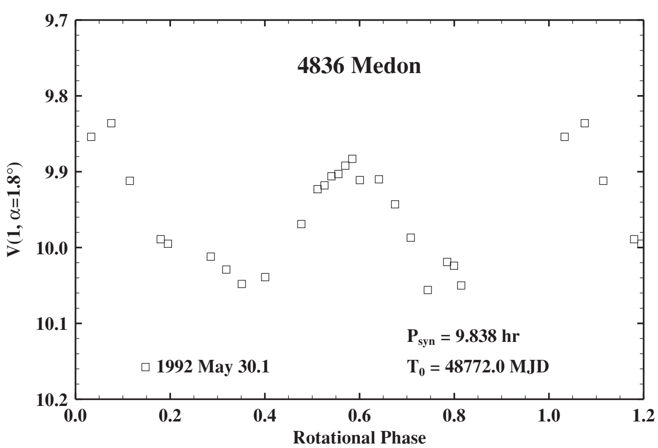

Figure 67. Composite light curve for 4836 Medon during the 1992 apparition.

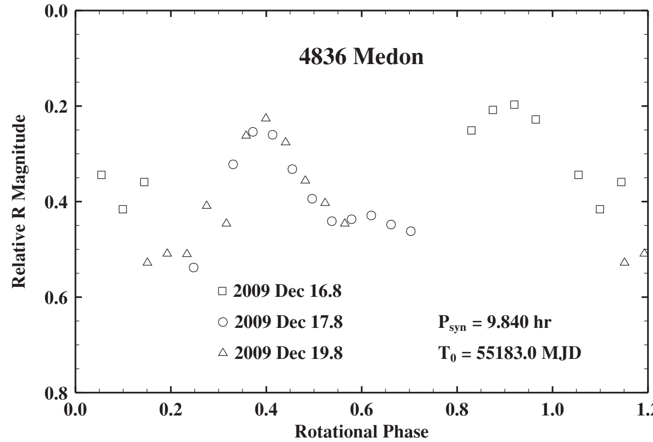

Figure 68. Composite light curve for 4836 Medon during the 2009 apparition.

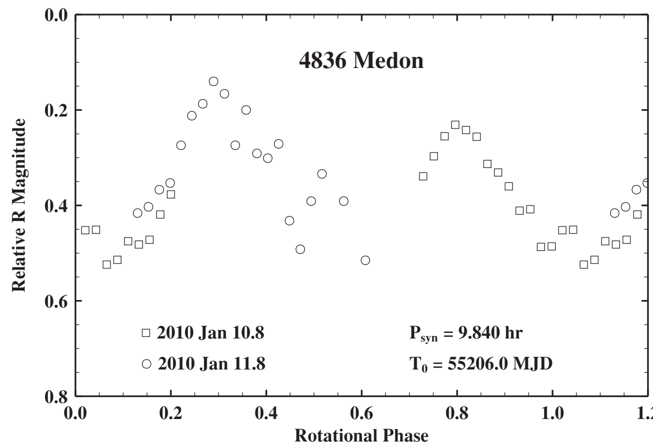

Figure 69. Composite light curve for 4836 Medon during the 2010 apparition.

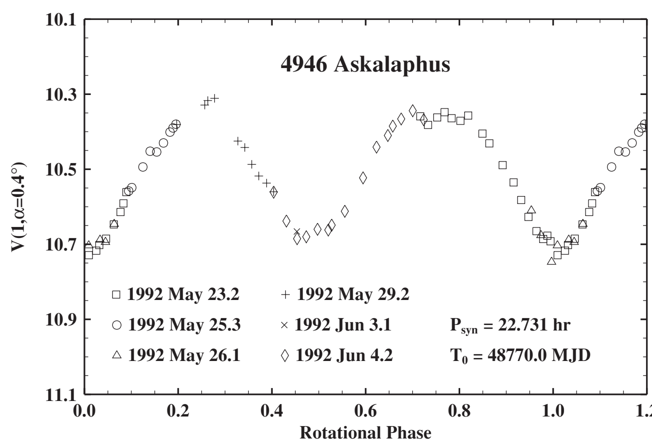

Figure 70. Composite light curve for 4946 Askalaphus during the 1992 apparition.

(see Figures 68 and 69), which confirmed the 9.84 hr period. No previous observations of this object are reported in the literature.

4946 Askalaphus

Askalaphus was observed during its 1992 apparition. After the first few nights it became apparent that the rotation period was close to 24 hr (see Figure 70). As a consequence, the following observations were carefully planned to allow for a complete coverage of the light curve. The resulting period is unambiguous and represents the first determination for this object published in the literature.

5023 Agapenor

We observed this object for five nights in 2009 September. The best-fit period is 5.4 hr, and the resulting light curve is characterized by the presence of very subtle secondary maxima, in addition to the primary ones (see Figure 71). A solution with exactly half the period, although formally less probable, could

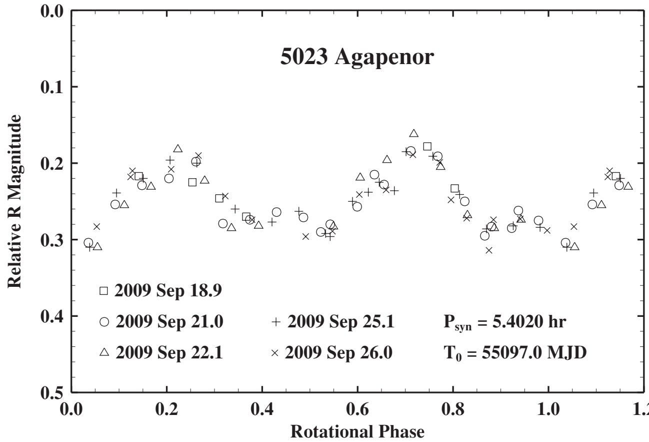

Figure 71. Composite light curve for 5023 Agapenor during the 2009 apparition.

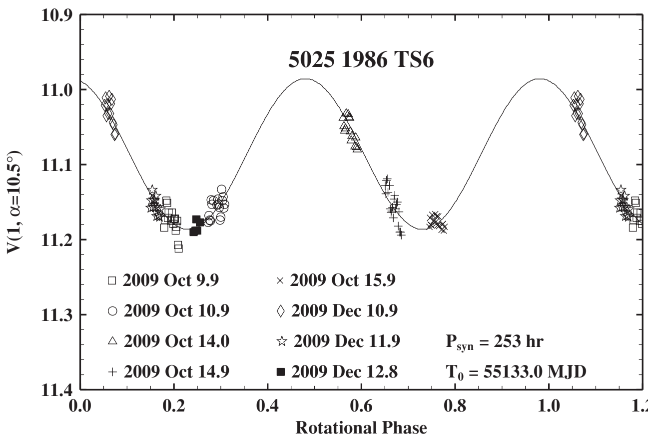

Figure 72. Composite light curve for 5025 1986 TS_6 during the 2009 apparition.

also be possible. This solution would result in a light curve with a primary maximum and a subdued secondary maximum. In order to resolve this ambiguity, observations from different geometries would be desirable, in order to monitor the evolution of the shape of the light curve as a function of the viewing direction. Should the shorter period be confirmed, this would represent the fastest rotator among the Trojans observed so far.

5025 1986 TS_6

This object was observed for eight nights during its 2009 apparition. During each night, mostly constant slopes were observed, with significant brightness variations from night to night, which was suggestive of a long period (see Figure 72). In order to estimate the rotation period, we fitted the data to a sine wave. We divided the observations into three groups of adjacent nights, where the observations within each group were referenced to the same set of in-field comparison stars. The fit, which involved solving for three parameters (two magnitude offsets and the period), results in a rotation period exceeding 10 days. Although this period requires confirmation, we believe that this object is among the slowest Trojans observed so far. In the case where 5025 has no companion, its rotation state might be excited, as the damping times for an object of this size are of the order of a few billion years (Harris 1994).

5027 Androgeos

Androgeos was observed for three nights during its 1992 apparition, which resulted in an unambiguous rotation period of 11.355 hr (see Figure 73). No other photometric measurements are reported in the literature for this object.

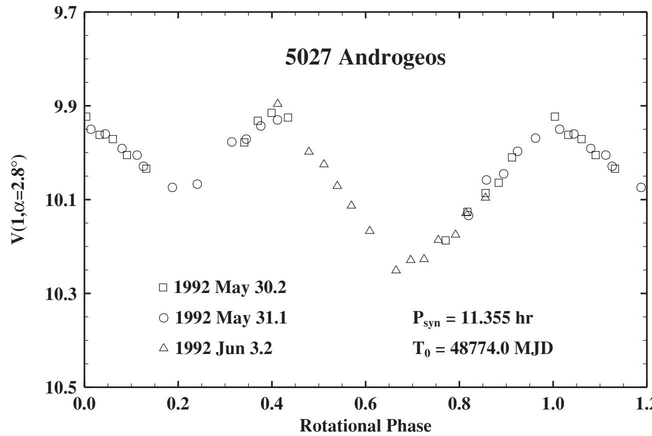

Figure 73. Composite light curve for 5027 Androgeos during the 1992 apparition.

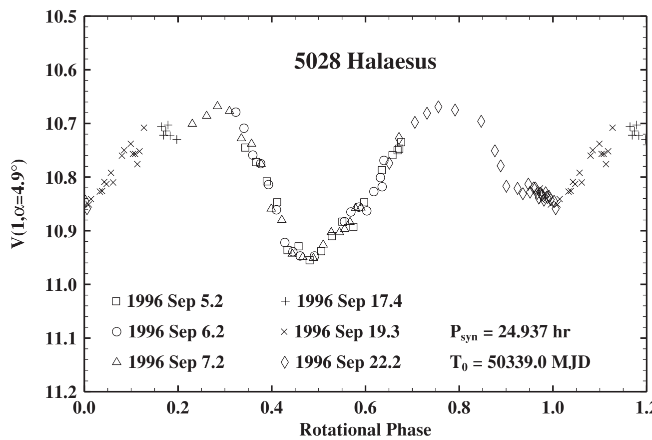

Figure 74. Composite light curve for 5028 Halaesus during the 1996 apparition.

5028 Halaesus

A reliable rotation period just under 25 hr was measured for this object in six nights of observations in 1996 (see Figure 74). This represents the only period determination available for this object in the literature.

5119 1988 RA_1

A literature search revealed no previous period determinations for this objects, for which we measured an unambiguous period of 12.807 hr during three nights of observations in 1992 (see Figure 75).

5120 Bitias

We observed Bitias during four consecutive nights in 1993 and derived a period of 11.58 hr. Since the period is close to 12 hr, however, we could only cover about 70% of the light curve (see Figure 76).

5130 Ilioneus

Five nights of observations in 1994 completely sampled the object's light curve multiple times, providing an unambiguous rotation period of about 14.8 hr (see Figure 77). No previous results have been published for this object.

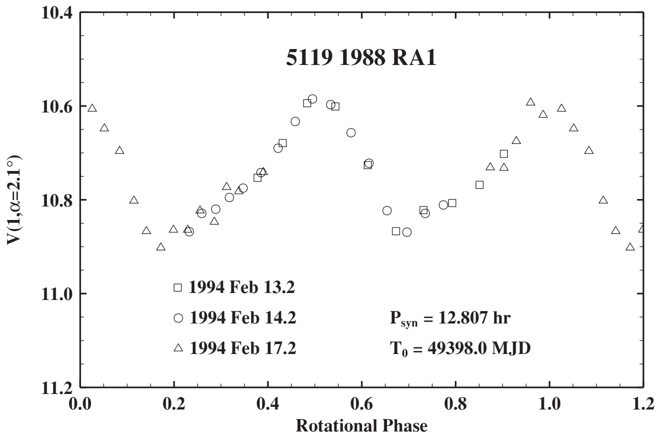

Figure 75. Composite light curve for 5119 1988 RA$_1$ during the 1994 apparition.

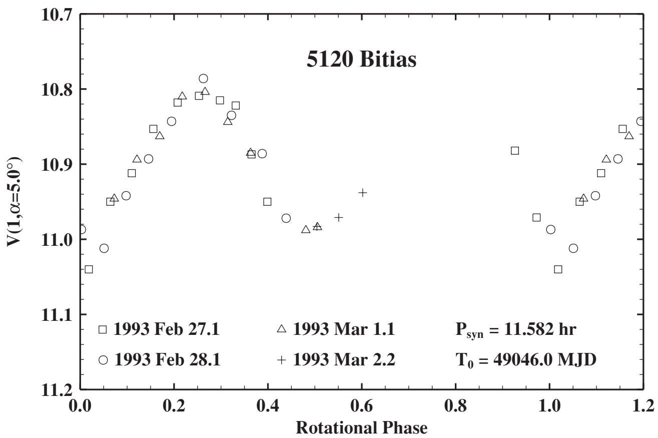

Figure 76. Composite light curve for 5120 Bitias during the 1993 apparition.

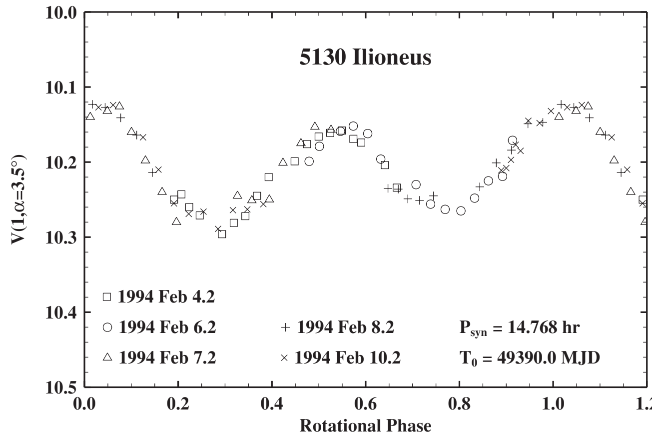

Figure 77. Composite light curve for 5130 Ilioneus during the 1994 apparition.

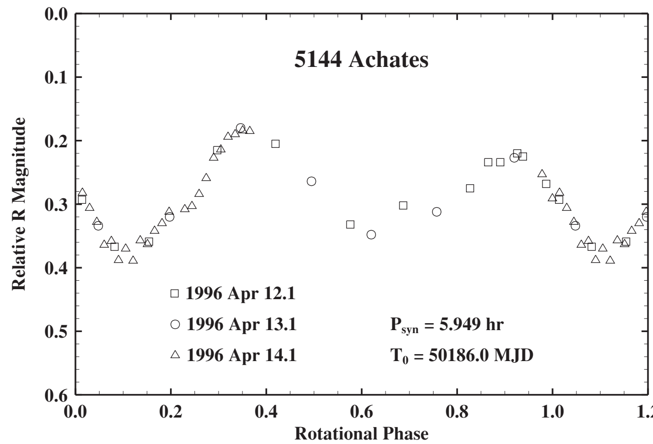

Figure 78. Composite light curve for 5144 Achates during the 1996 apparition.

5144 Achates

From three nights in April 1996 we derived a period of 5.949 ± 0.014 hr (see Figure 78), in good agreement with the recent determination by Molnar et al. (2008).

5254 Ulysses

Five nights of observations in 1996 completely covered its light curve, despite the relatively slow rotation (see Figure 79). We determine an unambiguous period of 28.72 hr, which represents the first period determination published for this object.

5259 Epeigeus

Five consecutive nights of observations in 1995 August resulted in a best-fit period of 18.51 hr for this object, which displays an irregular light curve with a comparatively low amplitude (see Figure 80).

5264 Telephus

Telephus was observed for four nights in 1994, yielding a reliable rotation period of 9.518 hr (see Figure 81), which represents the first period determination published for this object.

5283 Pyrrhus

We first observed this object during one night in 1996, when it showed very little light curve variation (see Figure 82). For this reason, we observed it again at our next opportunity, in 2002 March, when we could determine a reliable period of 7.323 hr (see Figure 83). We also used this period, which represents the first published determination for Pyrrhus, for plotting our observations of 1996, which turned out to cover the whole rotation in one night.

5476 1989 TO$_{11}$

Four nights of observations in 1994 revealed a regular light curve with moderate amplitude and an unambiguous period of 5.78 hr (see Figure 84), which represents the first period determination published for this object.

5511 Cloanthus

Observations during the 2010 apparition revealed only minor intensity variations during each individual night. The object, however, displayed large night-to-night variations, which hinted at a long rotation period. Thanks to the large detector field of view, it was possible to observe the same sets of in-field comparison stars during consecutive nights, which enabled us to accurately refer all of the observations to the same magnitude scale. Fitting a sine wave to the data results in a rotation period of about 14 days (see Figure 85). This object represents an interesting target for follow-up observations, being a potential complex rotator.

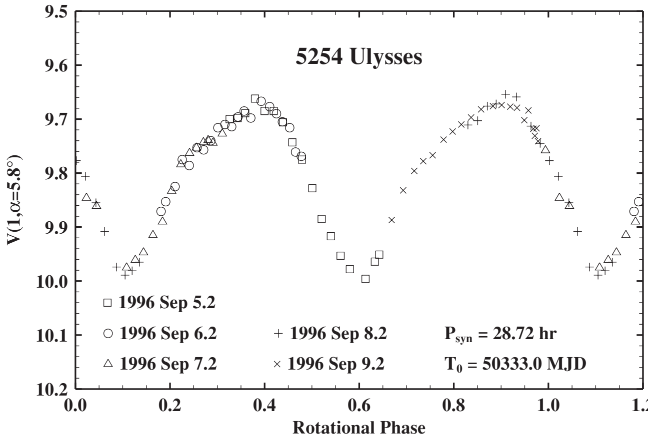

Figure 79. Composite light curve for 5254 Ulysses during the 1996 apparition.

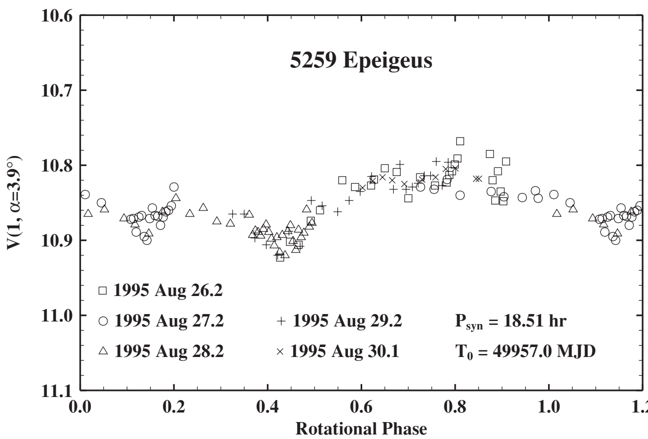

Figure 80. Composite light curve for 5259 Epeigeus during the 1995 apparition.

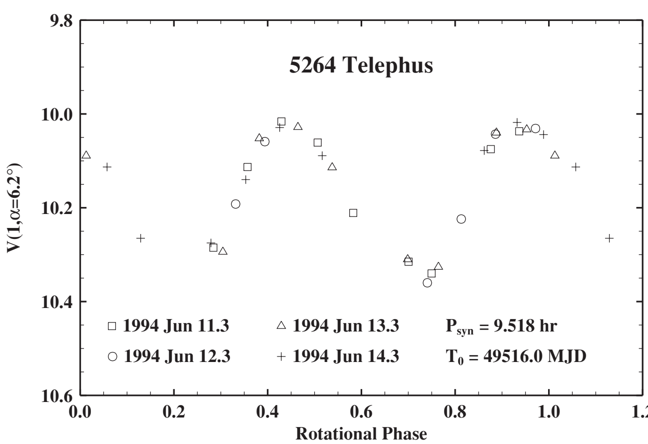

Figure 81. Composite light curve for 5264 Telephus during the 1994 apparition.

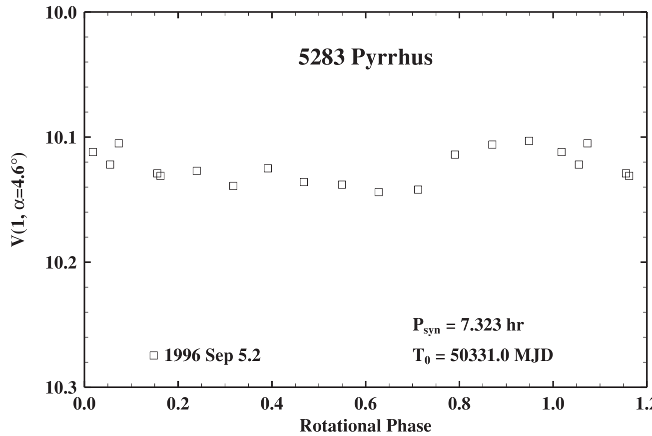

Figure 82. Composite light curve for 5283 Pyrrhus during the 1996 apparition.

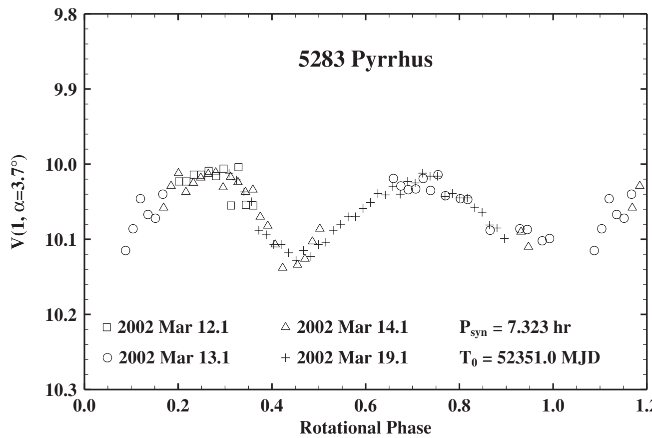

Figure 83. Composite light curve for 5283 Pyrrhus during the 2002 apparition.

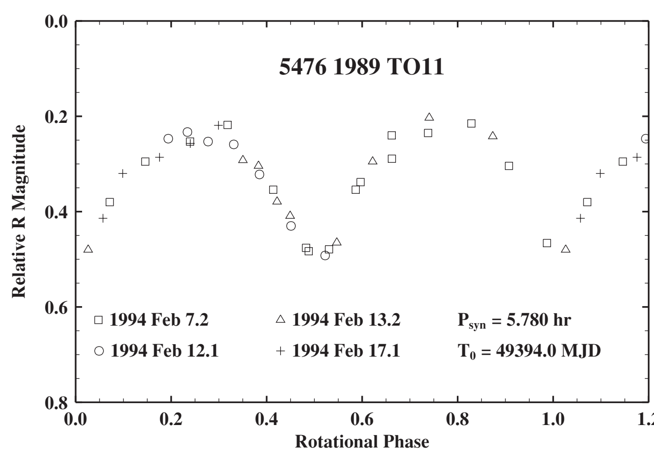

Figure 84. Composite light curve for 5476 1989 TO_{11} during the 1994 apparition.

5638 Deikoon

From six nights of observations in 1994 we derived a reliable rotation period of 9.137 ± 0.003 hr (see Figure 86). The object displays an irregular light curve with an amplitude of only 0.07 mag. Our determination rules out the tentative period published by Molnar et al. (2008).

5648 1990 VU_1

We observed this object for eight nights in 2009, which allowed us to determine an unambiguous period of 37.56 hr (see Figure 87). Despite the long rotation period, we covered about 80% of the rotation. Groups of two consecutive nights referred to the same in-field comparison stars. As a consequence, all observation groups share some overlap, and no arbitrary magnitude shift was used. Behrend (2010) reports on his Web page observations by Federico Manzini during three nights in the 2005 apparition; Manzini derived a rotation period of about 16 hr, which is incompatible with our determination.

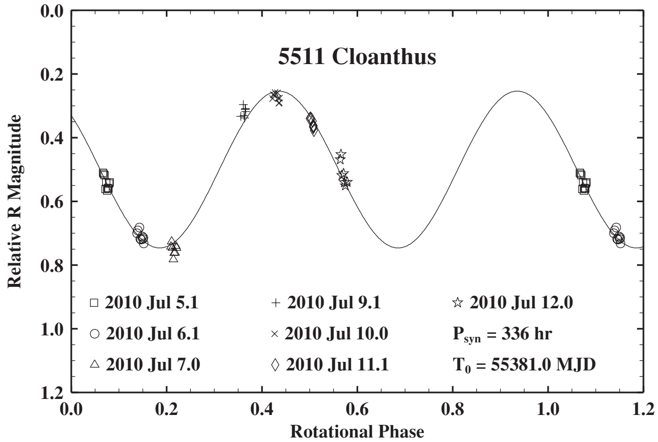

Figure 85. Composite light curve for 5511 Cloanthus during the 2010 apparition.

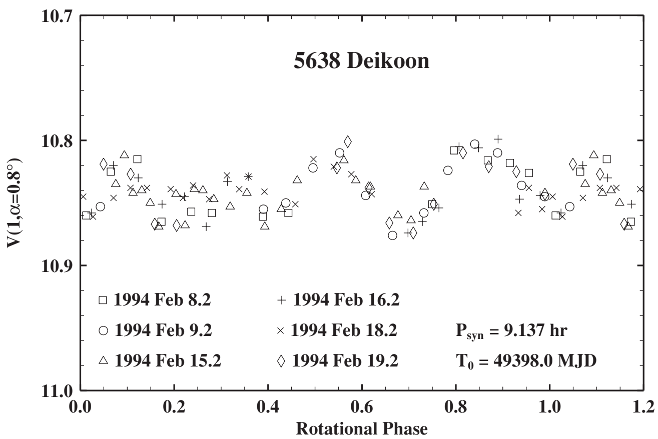

Figure 86. Composite light curve for 5638 Deikoon during the 1994 apparition.

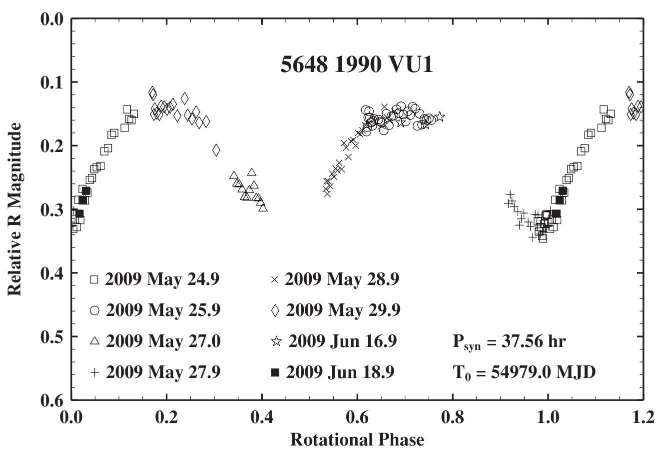

Figure 87. Composite light curve for 5648 1990 VU_1 during the 2009 apparition.

6002 1988 RO

Three nights of observations in 1993 February provided full coverage of the rotation of this object (see Figure 88). The period of 12.918 hr represents its first determination published in the literature.

6090 1989 DJ

Our first observations of this object, which were performed during five consecutive nights in 1994, revealed a very tortuous light curve with multiple features having a small amplitude

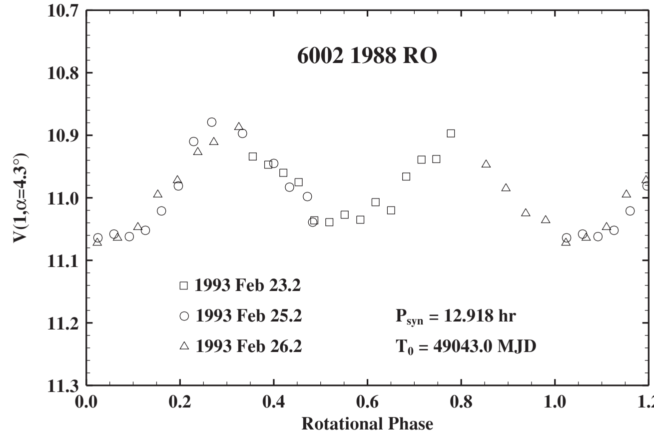

Figure 88. Composite light curve for 6002 1988 RO during the 1993 apparition.

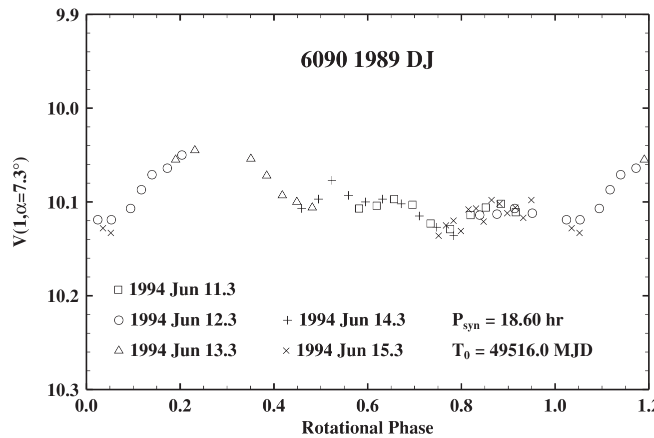

Figure 89. Composite light curve for 6090 1989 DJ during the 1994 apparition.

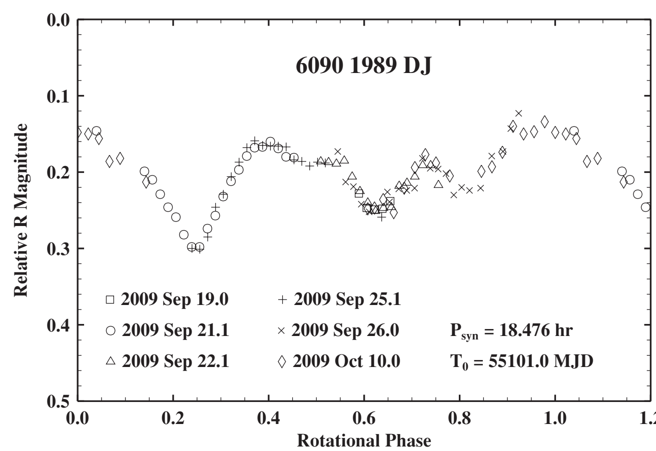

Figure 90. Composite light curve for 6090 1989 DJ during the 2009 apparition.

(see Figure 89). The best-fit period of about 18.6 hr produced excellent residuals, but was considered ambiguous because of the uncertain number of extrema occurring per cycle. Further observations, acquired during our next opportunity in 2009, captured a light curve with a higher amplitude, where the multiple features were easily identifiable across different cycles (see Figure 90). These observations allowed us to confirm our first determination of the rotation period.

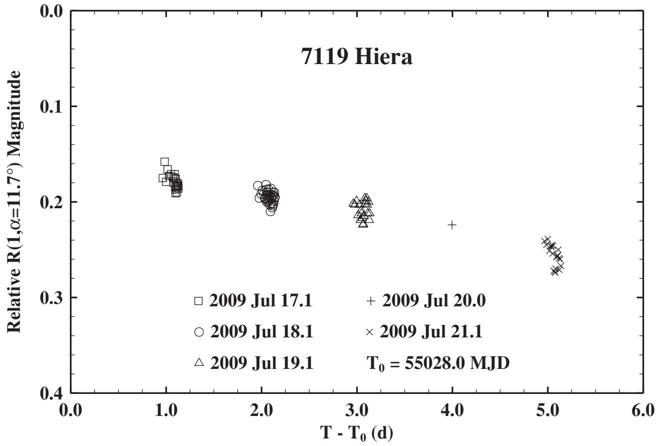

Figure 91. Individual light curves for 7119 Hiera during the July 2009 apparition.

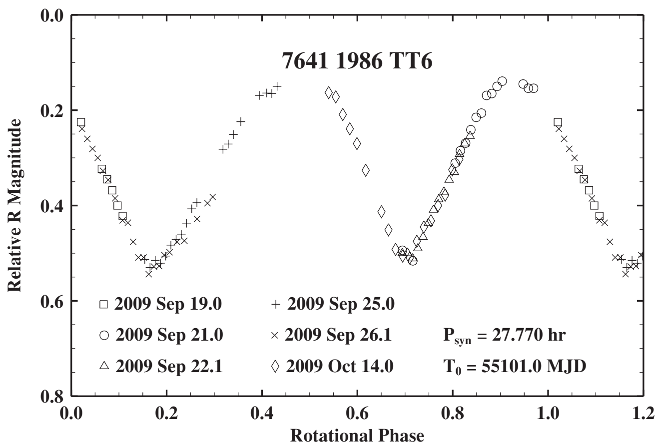

Figure 92. Composite light curve for 7641 1986 TT_6 during the 2009 apparition.

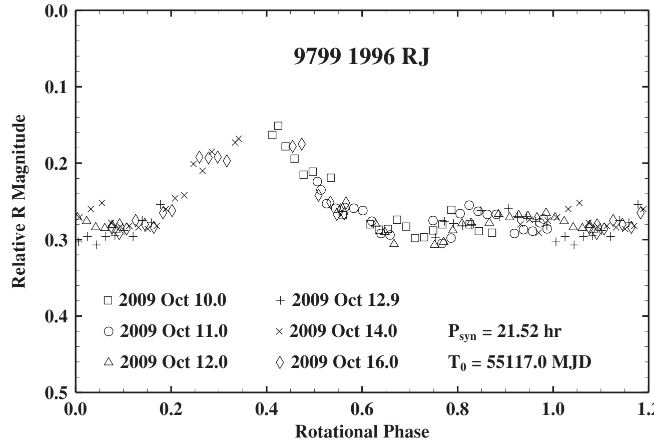

Figure 93. Composite light curve for 9799 1996 RJ during the 2009 apparition.

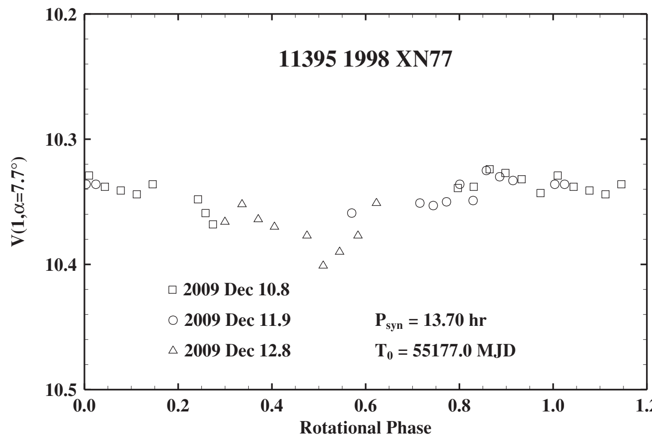

Figure 94. Composite light curve for 11395 1998 XN_{77} during the 2009 apparition.

7119 Hiera

We observed Hiera for five consecutive nights in 2009. The object displayed only very little variation during each single night. The night-to-night intensity, however, showed a gentle, systematic decreasing trend of about 0.1 mag over five days (see Figure 91), which was measured by referring the solar phase-corrected observations to the same sets of in-field comparison stars. We cannot completely rule out that such a trend of a few percent per day may be due to instrumental effects (as a systematic gradient in the flat fields would cause). However, should the observed light curve variation be confirmed to be solely due to the body's rotation, this would imply a rotation period longer than about 400 hr.

7641 1986 TT_6

Six nights of observations in 2009 completely covered the comparatively long rotation of this object (see Figure 92). A reliable period of about 27.8 hr represents the first determination published for this object.

9799 1996 RJ

We determined a reliable period of about 21.5 hr for this object from six nights of observations in 2009 (see Figure 93). The complete and multiple coverage of its single-peaked light curve makes the determination unambiguous.

11395 1998 XN_{77}

We first observed this asteroid for three consecutive nights in 2009 December. A first period search gave a result of 17.5 hr as the shortest possible period with a two-maximum, two-minimum light curve. Due to the low amplitude and the marginal overlap, however, we considered the period to be tentative. For this reason, this object was assigned a high priority on our target list, and was re-observed during the next opportunity in 2010 November for a total of seven nights (see Figure 95). The latter observations enabled us to determine an unambiguous synodic rotation period of about 13.7 hr. Re-analysis of the 2009 observations (see Figure 94) also showed the correct 13.7 hr solution, which was, however, previously discarded because it resulted in a single maximum–minimum light curve.

11509 Thersilochos

Six nights of observations in 2010 (see Figure 96) produced a well-sampled composite which resulted in an unambiguous synodic period of about 17.4 hr and which represents the first period determination published for this object.

12929 1999 TZ_1

From seven nights in 2009 May–June we derived a unique rotation period of 9.2749 ± 0.0016 hr (see Figure 97). Moullet et al. (2008) report previous optical observations for this object. From their sparse data set the authors suggest a period of 5.2 hr

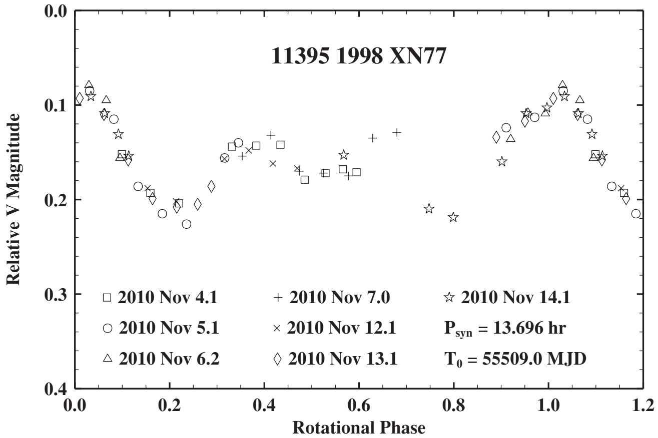

Figure 95. Composite light curve for 11395 1998 XN_{77} during the 2010 apparition.

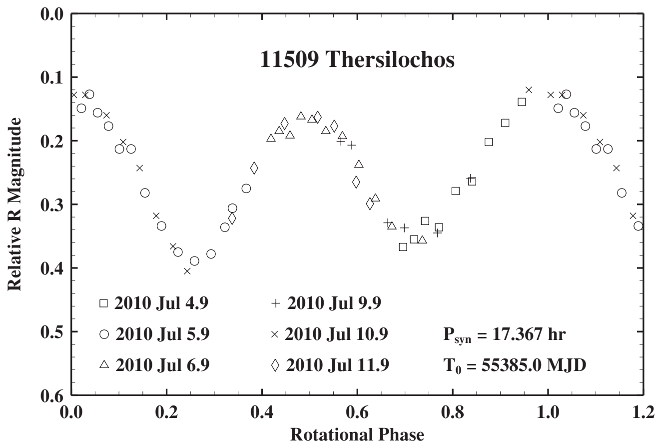

Figure 96. Composite light curve for 11509 Thersilochos during the 2010 apparition.

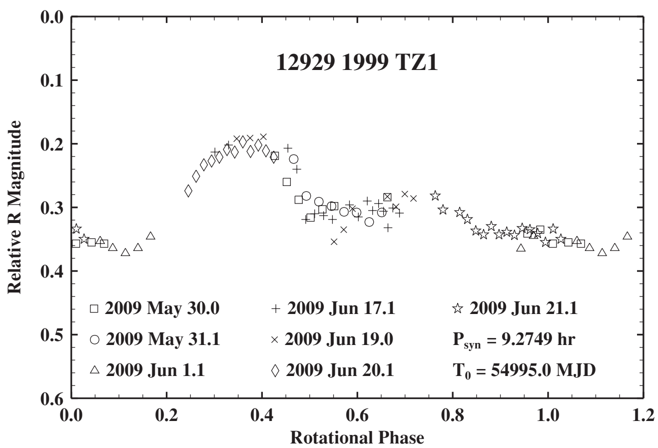

Figure 97. Composite light curve for 12929 1999 TZ_1 during the 2009 apparition.

or 10.4 hr, under the assumption of a single or double-peaked light curve, respectively. Neither period is, however, compatible with our data.

16974 1998 WR_{21}

Seven nights of observations in 2009 October unveiled a slow rotator with a period of about 3.3 days (see Figure 98). When compiling the composite, we linked consecutive nights which shared the same sets of in-field comparison stars. For this reason, although the composite covers about 75% of the whole rotation, all linked groups overlap, making arbitrary magnitude shifts unnecessary. This rotation period, which represents the first determination published for this object, is unambiguous.

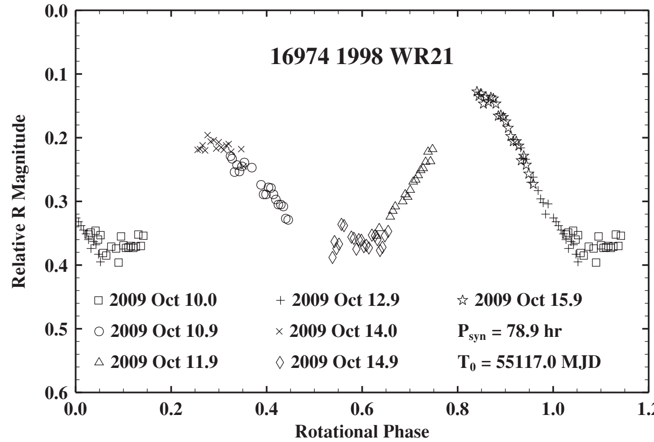

Figure 98. Composite light curve for 16974 1998 WR_{21} during the 2009 apparition.

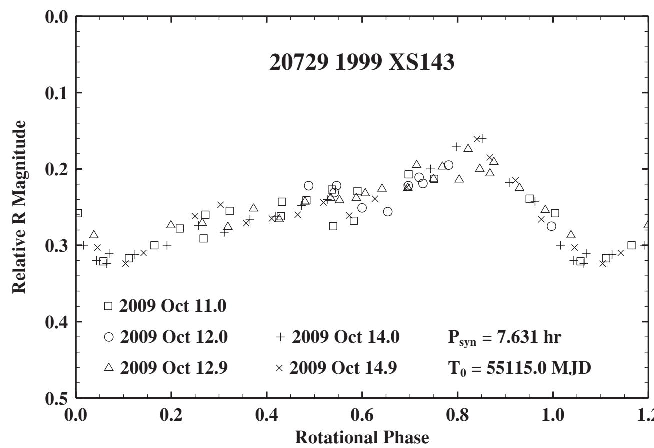

Figure 99. Composite light curve for 20729 1999 XS_{143} during the 2009 apparition.

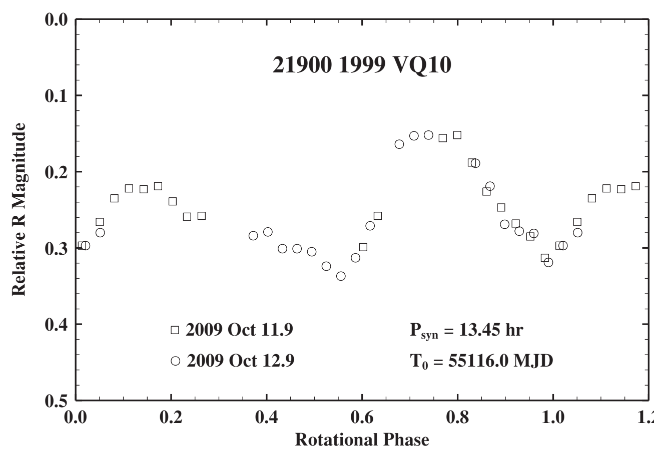

Figure 100. Composite light curve for 21900 1999 VQ_{10} during the 2009 apparition.

20729 1999 XS_{143}

This object was observed for five nights on 2009 October. During this apparition the light curve displayed a moderate amplitude and was characterized by a subdued secondary maximum and minimum (see Figure 99). From these observations we derive an unambiguous period of 7.631 hr.

Melita et al. (2010) report observations of this object performed for two consecutive nights in 2008 when the object showed a much higher amplitude. The authors reported a rotation period of 5.72 hr which is incompatible with our observations, and corresponds exactly to three fourths of the correct period. The probable reason for the disagreement is that the observations by Melita and coauthors, by covering only two time series of about 4.5 hr each, provide only incomplete coverage of the whole rotation. This led the authors to misjudge the number of rotation cycles between the two nights. By using the correct number of elapsed cycles (4), the observations by Melita et al. produce the correct period.

21900 1999 VQ_{10}

Two consecutive nights totaling about 18 hr of observations result in a rotation period of 13.44 ± 0.08 hr under the assumption of two maxima and two minima per cycle (see Figure 100). No previous observations of this object are reported in the literature.

5. SUMMARY

We have carried out a photometric survey of the rotational properties of Jupiter Trojan asteroids. The survey was designed to maximize the reliability of the determinations and to minimize observational bias. The latter was achieved by prioritizing observations of objects for which only inconclusive results were achieved. As a result, out of 80 Trojans observed, we derived new rotational periods for 56 objects, confirmed 13 previously published values, refined one period, and ruled out nine erroneous determinations. Although a thorough analysis of the rotational properties of the Trojans is the subject of a companion paper, we note that during our observations we recorded no extreme light curve amplitudes, with the largest being that of 3240 Lacoon with 0.55 mag. Furthermore, none of our objects showed a rotation faster than about 5.3 hr, a result that might have implications for the density, internal strength, and collisional evolution of these bodies. On the other hand, for about 5% of the objects we measured a period longer than 2 days, with two objects possibly showing a period longer than 14 days. Notwithstanding the considerable effort needed for observing these objects, it is fundamental to continue to follow up these slow rotators in order to understand the causes of their rotation state (Mann et al. 2007; Pravec & Harris 2000).

As a side note, we would like to mention that about 35% of the literature periods that we independently observed proved to be wrong. One possible way to improve this situation would be to re-establish an internet-based repository of light curve data similar to the Standard Asteroid Photometric Catalogue (Torppa 2008) with a user-friendly interface that would enable individual researchers to easily access and share light curve data and cross-check results (Stephens et al. 2010).

The authors are indebted to the many individuals who provided assistance over the years for the observations presented in this paper. In particular, we thank E. Braatz, E. Koldewey, E. Nagel, A. Nathues, G. Pupillo, and S. Hellmich for their help at the telescope. R. D. Stephens is gratefully acknowledged for providing us with his published observations of 4086 Podalirius in digital form.

REFERENCES

Angeli, C. A., Lazzaro, D., Florczak, A., Betzler, A. S., & Carvano, J. M. 1999, Planet. Space Sci., 47, 699
Barucci, M. A., Cruikshank, D. P., Mottola, S., & Lazzarin, M. 2002, in Asteroids III, ed. W. F. Bottke, Jr. et al. (Tucson, AZ: Univ. Arizona), 273
Beauge, C., & Roig, F. 2001, Icarus, 153, 391
Behrend, R. 2010, Observatoire de Geneve Web site, http://obswww.unige.ch/~behrend/page_cou.html
Binzel, R. P., & Sauter, L. M. 1992, Icarus, 95, 222
Bus, S. J., & Binzel, R. P. 2002, Icarus, 158, 146
Dell'Oro, A., Marzari, F., Paolicchi, P., & Vanzani, V. 2001, A&A, 366, 1053
Dell'Oro, A., & Paolicchi, P. 1998, Icarus, 136, 328
Dell'Oro, A., Paolicchi, P., Marzari, F., Dotto, E., & Vanzani, V. 1998, A&A, 339, 272
De Sanctis, M. C., et al. 1994, Planet. Space Sci., 42, 859
Duffard, R., et al. 2008, in Lunar Planet. Sci. Conf., 1405, Asteroids, Comets, Meteors 2008 (Houston, TX: LPI), 8187
Dunlap, J. L., & Gehrels, T. 1969, AJ, 74, 796
Fernandez, Y. R., Sheppard, S. S., & Jewitt, D. C. 2003, AJ, 126, 1563
Fowler, J. W., & Chillemi, J. R. 1992, in *IRAS* Asteroid Data Processing, The *IRAS* Minor Planet Survey, ed. E. F. Tedesco et al. (Technical Report PL-TR-92–2049; Hanscom AF Base, MA: Phillips Laboratory)
French, L. M. 1987, Icarus, 72, 325
Galad, A., & Kornos, L. 2008, Minor Planet Bull., 35, 144
Gonano, M., Di Martino, M., Mottola, S., & Neukum, G. 1991, Adv. Space Res., 11, 197
Harris, A. W. 1994, Icarus, 107, 209
Harris, A. W., et al. 1989, Icarus, 77, 171
Hartmann, W. K., & Tholen, D. J. 1990, Icarus, 86, 448
Hartmann, W. K., Tholen, D. J., Goguen, J., Binzel, R. P., & Cruikshank, D. P. 1988, Icarus, 73, 487
Jewitt, D. C., Trujillo, Ch. A., & Luu, J. X. 2000, AJ, 120, 1140
Lagerkvist, C.-I., Mottola, S., Carsenty, U., Hahn, G., Doppler, A., & Gnädig, A. 2000, in Minor Bodies in the Outer Solar System, ed. A. Fitzsimmons, D. Jewitt, & R. West (Berlin: Springer), 179
Lagerkvist, C.-I., & Sjölander, N.-G. 1979, Acta Astron., 29, 455
Landolt, A. U. 1983, AJ, 88, 439
Lasker, B. M., et al. 1988, ApJS, 68, 1
Lazzaro, D., Angeli, C. A., Carvano, J. M., Mothe-Diniz, T., Duffard, R., & Florczak, M. 2004, Icarus, 172, 179
Levison, H., Shoemaker, E. M., & Shoemaker, C. S. 1997, Nature, 385, 42
Mann, R. K., Jewitt, D., & Lacerda, P. 2007, AJ, 134, 1133
Marzari, F., Farinella, P., Davis, D. R., Scholl, H., & Campo Bagatin, A. 1997, Icarus, 125, 39
Melita, M. D., Duffard, R., Williams, I. P., Jones, D. C., Licandro, J., & Ortiz, J. L. 2010, Planet. Space Sci., 58, 1035
Milani, A. 1993, Celest. Mech. Dyn. Astron., 57, 59
Molnar, L. A., Haegert, M. J., & Hoogenboom, K. M. 2008, Minor Planet Bull., 35, 82
Mottola, S., De Angelis, G., Di Martino, M., Erikson, A., Hahn, G., & Neukum, G. 1995, Icarus, 117, 62
Moullet, A., et al. 2008, A&A, 483, L17
Pravec, P., & Harris, A. W. 2000, Icarus, 148, 12
Sato, I., Sarounova, L., & Fukushima, H. 2000, Icarus, 145, 25
Sauppe, J., Torno, S., Lemke-Oliver, R., & Ditteon, R. 2007, Minor Planet Bull., 34, 119
Shevchenko, V. G., et al. 2009, in 40th Lunar Planet. Sci. Conf. (Houston, TX: LPI), 1391
Stephens, R. D. 2009, Minor Planet Bull., 36, 59
Stephens, R. D. 2010, Minor Planet Bull., 37, 47
Stephens, R. D., Warner, B. D., & Harris, A. W. 2010, Abstract DPS 2010
Taylor, R. C. 1971, in Physical Studies of Minor Planets, ed. T. Gehrels (NASA SP-267; Washington, DC: NASA), 117
Tedesco, E. F., Noah, P. V., Noah, M., & Price, S. D. 2002, AJ, 123, 1056
Tedesco, E. F., Noah, P. V., Noah, M., & Price, S. D. 2004, *IRAS* Minor Planet Survey, IRAS-A-FPA-3-RDR-IMPS-V6.0. NASA Planetary Data System, (http://sbn.psi.edu/pds/resource/imps.html)
Torppa, J. 2008, http://www2.astro.helsinki.fi/SAPC/index.jsp
Warner, B. D., Harris, A. W., & Pravec, P. 2009, Icarus, 202, 134
Zappalà, V., et al. 1989, Icarus, 82, 354